Ace and *ace*-like genes of invasive redlegged earth mite: Copy number variation, target-site mutations, and their associations with organophosphate insensitivity

Joshua A Thia[1,*], Paul A Umina[1,2], Ary A Hoffmann[1]

[1] Bio21 Institute, School of BioSciences, The University of Melbourne, Melbourne, Victoria 3052, Australia

[2] Cesar Australia, Brunswick, Victoria 3056, Australia

[*] Corresponding author: josh.thia@live.com, joshua.thia@unimelb.edu.au

ORCID:

Joshua A. Thia https://orcid.org/0000-0001-9084-0959

Paul A. Umina https://orcid.org/0000-0002-1835-3571

Ary A. Hoffmann https://orcid.org/0000-0001-9497-7645

Keywords: Australia, non-convergent evolution, genomic outlier scans, pesticide resistance, pool-seq; whole-genome sequencing

Abstract

BACKGROUND. Invasive Australian populations of redlegged earth mite, *Halotydeus destructor* (Tucker), are evolving increasing organophosphate resistance. In addition to the canonical *ace* gene, the target gene of organophosphates, the *H. destructor* genome contains many radiated *ace*-like genes that vary in copy number and amino acid sequence. In this work, we characterise copy number and target-site mutation variation at the canonical *ace* and *ace*-like genes and test for potential associations with organophosphate insensitivity. This was achieved through comparisons of whole-genome pool-seq data from alive and dead mites following organophosphate exposure.

RESULTS. A combination of increased copy number and target-site mutations at the canonical *ace* was associated with organophosphate insensitivity in *H. destructor*. Resistant populations were segregating for G119S, A201S, F331Y at the canonical *ace*. A subset of populations also had copy numbers of canonical *ace* >2, which potentially helps over-express proteins carrying these target-site mutations. Haplotypes possessing different copy numbers and target-site mutations of the canonical *ace* gene may be under selection across *H. destructor* populations. We also detected some evidence that increases in copy number of radiated *ace*-like genes are associated with organophosphate insensitivity, which might suggest potential roles in sequestration or breakdown of organophosphates.

CONCLUSION. Different combinations of target-site mutations and (or) copy number variation in the canonical *ace* and *ace*-like genes may provide non-convergent ways for *H. destructor* to respond to organophosphate selection. However, these changes may only play a partial role in organophosphate insensitivity, which appears to have a polygenic architecture.

Introduction

Pesticide resistance in arthropod pests has been extensively studied to understand the genetic basis of adaptation to toxins. Many pesticides exert their toxicity through very specific structural interactions with a target protein (e.g., Russell *et al.*, 2004; Davies *et al.*, 2007; Crossthwaite *et al.*, 2014). Such precise biomolecular interactions commonly produce convergent evolution of the same mutations in the target gene ('target-site mutations') that confer pesticide resistance [4–6]. This observed convergence in target-site mutations is striking because it occurs across diverse taxonomic levels. For example, the target gene of organophosphate pesticides is the enzyme acetylcholinesterase (*ace*), which is responsible for breaking down to acetylcholine in the synapse [2]. Organophosphorus pesticides inhibit this action by competitively binding to *ace*, preventing acetylcholine breakdown, leading to uncontrolled firing at the synapse and ultimately death [7]. Many arthropod pests have evolved the same mutations that disrupt inhibition of *ace* by organophosphates, a convergence on the exact same genetic mechanism underpinning resistance (reviewed in: Fournier, 2005; Feyereisen *et al.*, 2015).

However, the genetic basis of pesticide resistance can be more complex than mutational changes in target sites. Duplications of target genes can contribute to resistance by increasing gene dosage, elevating the number of target protein molecules that must be bound by a pesticide to achieve mortality (Kwon, Clarkt, & Lee, 2010; Deok Ho Kwon, Choi, Je, & Lee, 2012). Target gene duplications can also propagate haplotypes

carrying target-site mutations in the genome, increasing the proportion of target protein molecules carrying pesticide resistance mutations (Carvalho et al., 2012; Kwon et al., 2010). Alternatively, increased expression of duplicated target genes may be beneficial because a comparable level of enzymatic activity is retained despite reduced functionality of resistant proteins [10]. Target-site mutations can, however, come with considerable fitness costs [13,14]. Other genes unrelated to target-sites can also contribute to pesticide resistance, including genes involved in detoxification processes [15–17], and (or) genes that help reduce cuticle penetration by pesticides [15,18].

In this study, we focus on the redlegged earth mite, *Halotydeus destructor* (Tucker 1925; Penthaleidae, Trombidiformes), an agricultural pest mite of Australian grain and pasture crops. This mite invaded the state of Western Australia from South Africa around 1917 and spread throughout the southern regions of Australia during the 1920s (Newman, 1925; reviewed by Ridsdill-Smith, 1997). It is a winter-active pest, which diapauses as eggs during the Australian summer (October–March), emerges in autumn (April–May), and typically undergoes its active life stage through to late spring (April–November) [20]. Control of this mite for many decades has been largely achieved through the application of pyrethroid and organophosphate pesticides [21,22]. Low-level tolerance to these pesticides was initially observed in the 1990s and early 2000s [23,24], with high-level pyrethroid resistance first detected in field populations in 2006 [25] and organophosphate resistance first detected in 2014 (Umina et al. 2017).

Whilst the molecular mechanism of pyrethroid resistance in *H. destructor* has mostly been linked to target-site mutations [26–28], the molecular mechanism of organophosphate resistance has been difficult to elucidate. We recently assembled a draft genome for *H. destructor*, which helped reveal a large radiation event in *ace*-like genes [29]. Our previous comparative analyses showed that such a radiation of *ace*-like is highly unusual among other arthropod pests but has also been observed in *Tetranychus urticae*, the two-spotted mite, another problematic trombidiform mite pest [29]. There are some 28 distinct genes, which we refer to as the canonical *ace* gene or *ace*-like genes in the *H. destructor* genome. The protein products of these genes vary in size from 231–1096 amino acids in length; typically, *ace* genes are around 600 amino acids long and the standard reference from *Torpedo californica* is 596 amino acids long (GenBank: X03439.1).

We had previously reported the presence of known organophosphate target-site mutations (G119S, A201S, and F331Y) in the canonical *ace* gene [29] that are segregating in resistant populations. However, the amino acid sequence variation in the radiated *ace*-like genes has yet to be formally characterised. We also suspect that the canonical *ace* and ace-like genes may vary in copy number [29]. The exact functional roles of radiated *ace*-like genes in *H. destructor* are currently unknown. However, if some of these *ace*-like genes can bind organophosphates, they could help reduce inhibition of canonical *ace* activity by sequestering pesticide molecules [30]. Organophosphates may also select for mutations in esterases that allow them to hydrolyse organophosphates, reducing inhibition of canonical *ace* activity through metabolism of pesticide molecules [31]. If any of these radiated *ace*-like genes can contribute to organophosphate insensitivity, there may be diverse ways in which they could combine with the canonical *ace* to influence the phenotypes of *H. destructor* (Figure 1).

In this study, we characterised copy number variation and target-site amino acid variation in the *ace* and *ace*-like genes of *H. destructor* and test for associations with organophosphate insensitivity. We also explored the role of other non-*ace* genes in responses to organophosphates. We used a pool-seq approach to obtain whole-genome data from mites that were alive (insensitive) and dead (sensitive) following organophosphate

exposure. These mites came from populations with different levels of evolved organophosphate resistance. Our results are most consistent with a possible combinatorial mechanism of resistance by which different combinations of target-site changes and (or) copy number variation in *ace* and *ace*-like genes may contribute to organophosphate insensitivity in *H. destructor*. However, these effects are variable across populations and they can be small, suggesting that organophosphate insensitivity often has a polygenic architecture which also encompasses other mechanisms. The potential polygenicity of organophosphate insensitivity was evident from a lack of clear signals of selection in genomic outlier scans. These findings suggest non-convergent evolution of organophosphate resistance across populations.

Methods

Terminology and definitions

Organophosphate insensitivity. An individual (or population) is typically considered 'resistant' to a pesticide when it has evolved to survive exposure to high chemical doses. In contrast, 'susceptible' individuals (or populations) are those that have not evolved resistance and are killed at doses that otherwise 'resistant' individuals (or populations) would survive at. At a high exposure dose, the nomenclature 'resistant' versus 'susceptible' is intuitive but is more subjective when high doses cannot be tolerated, and (or) if a low exposure dose is used. We therefore use the term 'organophosphate insensitivity' in this study as a more general way of separating individuals exposed to pesticide from populations with different phenotypic means. Here, individuals within populations that could survive organophosphate exposure are considered 'insensitive', whereas those that were killed by exposure are considered 'sensitive'. This definition allows us to refer to responses of phenotypically 'resistant' and 'susceptible' populations more generally.

***Ace* and *ace*-like genes.** We use the term '*ace*-like' for annotated genes with similar sequences to *ace* that appear to have radiated in the *H. destructor* genome. These radiated *ace*-like genes are all divergent from the 'canonical *ace*' gene, the putative functional version of *ace* that is orthologous to those in other arthropods [29]. Although we are yet to determine the functional characteristics of the radiated *ace*-like genes, we hypothesize some may contribute to organophosphate insensitivity through different potential mechanisms (Figure 1). We consider that the canonical *ace* gene and radiated *ace*-like genes exist as their own lineage. This is an important definition because we show in this study that each unique *ace* or *ace*-like gene can possess copy number variation within and among populations. In this work, we focus on the canonical *ace* gene and 18 focal *ace*-like genes that reside on large genomic contigs (see below). We refer to these genes by annotation codes, 'HDE_X', where 'X' is a unique gene number.

Biological material

Halotydeus destructor collected for this study came from industry projects surveying phenotypic resistance in the states of Western Australian and Victoria (Figure 2) (described in Thia et al., 2023). All Western Australia populations (Manjimup, Tambellup, Treeton, and Yongarillup) were found to be resistant to organophosphates. Victoria populations included two from Colbinabbin, one with evolved resistance to organophosphates (herein referred to as Colbinabbin Res) and the other susceptible to organophosphates (herein referred to as Colbinabbin Sus). A third Victorian population was collected from Wantirna South and previously used to

assemble the reference genome for *H. destructor* [29]. Although not phenotypically screened in this study, mites from Wantirna South are known to be susceptible to organophosphates.

Collections of mites from phenotypic resistance surveys were exposed to either omethoate (Western Australia populations) or dimethoate (Victoria populations), two widely used organophosphates for mite control in Australia. The Western Australian mites used in this study were exposed to either 5.8 or 8.7 mgL^{-1} omethoate; 5.8 mgL^{-1} is a standard discriminating omethoate dose for resistance in *H. destructor* that kill phenotypically susceptible mites [21]. Colbinabbin Res mites were exposed to 34 mgL^{-1} of dimethoate, and Colbinabbin Sus mites were exposed to 3.4 mgL^{-1} dimethoate. These doses produce roughly 60% mortality in their respective populations, and all mites from the Colbinabbin Sus population die at 34 mgL^{-1} (Joshua Thia, personal communication). Pesticide exposures were implemented using the coated vial method [21,24,25]. Briefly, mites were collected from the field and held at 4°C before exposure to pesticide. Pesticides were prepared by diluting stock solutions of 290 gL^{-1} omethoate (Le Mat®) or 400 gL^{-1} dimethoate (ADAMA®) in distilled water with 0.01% polysorbate 80 (Tween®), and then diluted to make up the necessary doses. Pesticides were swirled in 30 mL plastic vials to coat and left to air-dry overnight. The following day, around 50 mites were placed into the vials along with a single vetch (*Vicia sativa*) leaf. After 24 h at 18°C, mites were scored as alive (insensitive) and dead (sensitive) following Hoffmann et al. (1997). These mites were then separated, placed into Eppendorf tubes with 100% ethanol and frozen at −20°C prior to molecular analysis. For some populations, we also kept samples of untreated mites that were either unexposed to pesticides (Colbinabbin Res and Colbinabbin Sus) or were exposed to a dose that imposed 0% mortality (Manjimup to 0.87 mgL^{-1} omethoate).

Pool-seq library preparation

Alive and dead mites were used to create pooled DNA extractions using a DNeasy® Blood and Tissue Kit (Qiagen, Hilden, Germany). Each DNA extraction represented a unique biological replicate comprising 10–70 mites (see Table S1). For each DNA extraction, two 150 bp paired-end whole-genome Illumina short-read libraries were constructed by Novogene (Novogene Co. Ltd, Hong Kong), which represented technical replicates of each pooled DNA extraction. Pool-seq libraries were generated for at least one pool of alive and dead mites for all populations, except Wantirna South for which we had a single untreated collection. We also produced pool-seq libraries for untreated mites from Colbinabbin Res, Colbinabbin Sus, and Manjimup.

For downstream analysis, pool-seq libraries were aggregated to different levels. For each unique DNA pool, we always aggregated replicate pool-seq libraries. In the Manjimup and Yongarillup samples, we also aggregated different DNA pools from the same population and pesticide treatment to increase the number of pooled diploid individuals. We initially extracted DNA from smaller pool sizes to increase biological replication from available mite collections. We indicate the aggregation of DNA pools from the same population and pesticide treatment in Table S1. Herein, we refer to 'samples' as sets of aggregated DNA pools. Samples were used to establish contrasts between alive and dead mites. All populations were represented by one alive–dead pair of samples, except the Colbinabbin Res and Sus populations, for which we had two independent pairs. For the Colbinabbin Res and Sus populations, we also included a pair of untreated samples. Details of sample contrasts are provided in Table 1.

Bioinformatic processing and SNP variant calling

Raw reads for each unique pool-seq library were quality trimmed using FASTP [32], truncating reads to 100 bp and discarding all reads below this threshold. Trimmed reads for each pool-seq library were mapped to the *H.*

destructor reference genome (GenBank GCA_022750525.1) using BOWTIE2 [33] with a global alignment and the '--sensitive' mapping option. Following trimming, our FASTQ files for individual pool-seq libraries contained a mean of 29,570,401 reads with a range of 21,791,964–41,049,660 reads. The mean number of reads mapping to the *H. destructor* genome (genomic contigs >0.2 Mb) was 15,522,450 reads with a range of 11,132,739–23,519,859 per individual pool-seq library. Mapping was limited to contigs >0.2 Mb in length because our prior study identified that mapping to contigs <0.2 Mb led to variable and unreliable mapping [29]. SAMTOOLS [34,35] was used to discard reads with mapping quality <30 and those that were found to be PCR duplicates. Variant calling was performed using FREEBAYES [36] with the arguments: '--min-alternate-count 3' and '--pooled-continuous'. The FREEBAYES script, *fasta_generate_regions.py*, was used to segment the genome for variant calling in parallel. We used BCFTOOLS [34,37] to combine VCF files from across the parallel variant calling runs. Variant filtering was performed with VCFTOOLS [38] to retain only single nucleotide polymorphisms (SNPs; no indels) with a minor allele count of 3, a minor allele frequency of 0.01, minimum quality of 30, minimum depth of 20 reads per sample, no missing data, and to exclude SNPs from repetitive regions of the genome.

Ace copy number variation

We estimated a proxy for copy number at the canonical *ace* and *ace*-like genes using whole-genome data. These estimates of copy number were then used to test the hypothesis that greater copy number is associated with organophosphate insensitivity in *H. destructor*. Our proxy for copy number at the canonical *ace* or *ace*-like genes was derived from read depth ratios relative to 866 single copy reference genes that were verified in prior BUSCO analyses [29]. These single copy reference genes all resided on genomic contigs >0.2 Mb in length. We extracted mean read depth information for these single copy reference genes, the canonical *ace*, and 18 *ace*-like genes with the SAMTOOLS COVERAGE function. Read depth statistics were then imported into R v4.1.3 [39] for further analysis.

We first summarized read depth for the canonical *ace*, the 18 focal *ace*-like genes, and the 866 single copy reference genes as the mean across replicates libraries nested in pools nested in samples (Table S1). We then obtained read depth ratios in the canonical *ace* or *ace*-like genes as a proxy for copy number by dividing their read depth by that of each single copy reference gene. The *ace* and *ace*-like genes were distributed across 11 genomic contigs, and the single copy reference genes were distributed across 52 genomic contigs. All genomic contigs containing the focal canonical *ace* and *ace*-like genes were represented in contigs containing single copy reference genes. This meant we were able to incorporate genome-wide variation in read depth into our formal hypothesis using a mixed effects linear model:

Ace depth ratio = Survival + State|Population + *Ace* gene + Reference gene

In this model, the response '*Ace* depth ratio' is the read depth ratio for the canonical *ace* or *ace*-like genes. 'Survival' is the survival status, a categorical fixed effect, alive or dead. We fitted the random intercepts for 'Population' nested within 'State' of sample origin, and separate random intercepts for the canonical *ace* or *ace*-like genes, '*Ace* gene', and each single copy reference gene, 'Reference gene'. The model was fitted using the LME4 [40] and LMERTEST [41] R packages. We calculated the mean difference in depth ratio across *ace* genes to summarise differences in depth ratio between alive and dead mites.

Ace target-site mutations

We surveyed the canonical *ace* and *ace*-like genes for polymorphisms at codons known to be associated with target-site resistance in other arthropods: 73, 78, 82, 119, 128, 129, 150, 201, 201, 227, 280, 290, 328, 330, 331, 336, 435, and 441 (*Torpedo californica* numbering) (reviewed in: Fournier, 2005; Feyereisen *et al.*, 2015). We used our alignment of *H. destructor ace* protein sequences with *T. californica* to determine the homologous codon positions in *H. destructor*. We then identified the underlying nucleotide bases for each codon and determined whether any of our SNPs were associated with these a priori codons. We surveyed the 19 *ace* genes residing on genomic contigs >0.2 Mb in length. To further explore the distribution of amino acid polymorphisms, we examined the read alignments in a subset of pool-seq libraries. We extracted mapped reads from select libraries from Wantirna South, Colbinabbin Sus, Colbinabbin Res, and Manjimup populations using the GENOMICALIGNMENTS [42] and BIOSTRINGS [43] R packages.

After identifying non-synonymous SNPs in the a priori target-site codons, we tested whether polymorphisms at these SNP were associated with organophosphate insensitivity. We compared the allele frequencies between alive and dead mites using a X^2 test of the observed read counts for the reference and alternate allele (a two-by-two contingency table). We calculated the frequency differential between treated alive and dead mites (or between untreated samples) in each sample pair (Table 1) by subtracting the reference allele frequency of dead mites from that of alive mites (or one untreated sample from another).

Genomic outlier scan

We used our whole-genome data to perform a scan for outlying genomic regions that may exhibit signatures of organophosphate selection when comparing alive and dead mites. The purpose of this analysis was two-fold: (1) to provide additional support for the contributions of the canonical *ace* or other *ace*-like genes to organophosphate insensitivity; and (2) to identify other non-*ace* genes that may contribute to organophosphate insensitivity. We measured genetic differentiation between alive and dead mites using the mean F_{ST} for a genomic region ('blocks'). We aggregated pool-seq libraries to generate reference and alternate allele read counts for working sample pairs in R (Table 1). We used the POOLFSTAT R package to filter SNPs. For each working sample pair, SNPs were filtered at a minor allele frequency threshold of 0.1. We then defined SNP blocks as genomic regions comprising 30–50 SNPs, resulting in a median SNP block size of 6,040 bp, and a range of 1,022–82,863 bp. We also performed these same tests on untreated sample pairs to infer the stochastic background differentiation expected.

To calculate the mean F_{ST} for a genomic region, we first calculated SNP-wise estimates of F_{ST} 'corrected' for sample size and technical error using POOLFSTAT:

$$F_{ST} = \frac{Q_1 - Q_2}{1 - Q_2}$$

Here, Q_1 is the identity in state probability for two genes sampled within a population pool, and Q_2 is the identity in state probability for two genes sampled between two population pools. This formulation is equivalent to ϑ, as defined by Weir & Cockerham's (1984). We also calculated an 'uncorrected' F_{ST} [44]:

$$F_{ST} = \frac{\sigma}{\bar{p}(1-\bar{p})},$$

where σ is the variance in the reference allele frequency and $\bar{p}$ is the mean reference allele frequency. After calculating SNP-wise estimates of F_{ST}, we calculated block-wise F_{ST} by dividing the mean numerator by the

mean denominator variance components for all SNPs within a block. We therefore had block-wise F_{ST} estimates corrected and uncorrected for sample size and technical error. SNP blocks exhibiting unusually high genetic differentiation were identified using a two-step method. The uncorrected block-wise F_{ST} values were subjected to the algorithm described in the OUTFLANK method [45] to identify a set of 'preliminary' outlier blocks. To execute the OUTFLANK method, we used a hybrid script comprised of custom code and functions borrowed from the OUTFLANK GitHub (used to calculate effective degrees of freedom and the two-sided X^2 test-statistic *p* value) [46]. The preliminary outlier blocks were retained if they exceeded the 99th percentile calculated from corrected block-wise F_{ST} values. Those blocks passing both steps comprised our 'final' outlier blocks.

Genes residing in the final outlier blocks were considered candidate genes of organophosphate insensitivity. To test whether certain types of genes were over-represented in this candidate gene set, we used a gene ontology (GO) enrichment analysis. GO enrichment was analyzed using Fisher's exact tests in R. The significance of enrichment was assessed following Bonferroni correction of *p* values.

Results

Ace copy number variation

We found support for our hypothesis that greater copy numbers of the canonical *ace* and *ace*-like are associated with organophosphate insensitivity, but the role of copy number may vary by gene and (or) population. Most genes had read depth ratios that were distributed around 1.00, suggesting they existed largely as single copies, but a few genes had depth ratios that deviated notably from 1.00 in some or all samples (Figure 3). In the canonical *ace*, HDE_14279, samples from three Western Australia populations, Manjimup, Treeton, and Yongarillup had depth ratios ranging from 1.49–2.37, suggesting a much higher average copy number in these populations. In contrast, several *ace*-like genes had depth ratios <1.00 across all samples, suggesting that these genes might not be present in every genome: HDE_12794 (0.55–0.86), HDE_09715 (0.16–0.50), HDE_09713 (0.36–0.64), HDE_09712 (0.53–0.82), and HDE_09711 (0.73–0.91).

Our linear mixed effects model of read depth ratio identified a significant fixed 'Survival' effect ($F_{1,196558}$ = 749.13, $p < 0.001$), but the overall effect was small (β_{Dead} = –0.02, t = –27.37, df = 196558, $p < 0.001$). On average, alive mites had a read depth ratio of 0.91 (±0.06 SE), whereas dead mites on average had a read depth ratio of 0.89 (± 0.0007 SE). We also reran the model excluding the canonical *ace* gene to check that it was not biasing results. There was still an overall positive association between copy number in *ace*-like genes and survival following organophosphate exposure ($F_{1,186167}$ = 390.46, $p < 0.001$), although the effect size was smaller after removing the canonical *ace* (β_{Dead} = –0.007, t = –19.76, df = 1861670, $p < 0.001$). The mean difference in depth ratios between alive–dead pairs were positive for the Colbinabbin Res (0.09 ± 0.01 SE), Colbinabbin Sus (0.07 ± 0.01 SE), Treeton (0.04 ± 0.02 SE), and Yongarillup (0.09 ± 0.01 SE) populations. In contrast, the mean difference in depth ratios was negative for the Manjimup (–0.05 ± 0.03 SE) and Tambellup (–0.05 ± 0.02 SE) populations. These results suggest that at least some *ace*-like genes may have subtle contributions to organophosphate insensitivity through small variations in copy number. In a subset of populations, a more discernible increase in copy number in the canonical *ace* gene is linked to organophosphate insensitivity, which may help over-express resistant proteins (see below).

Ace target-site mutations

Among our 19 focal genes and 19 a priori *ace* target-sites codons surveyed, only 6 non-synonymous SNPs were identified across all samples (Table 2). One SNP was observed in the *ace*-like HDE_01555, a L331M mutation; one SNP was observed in *ace*-like HDE_01576, a R238K mutation; and four SNPs were observed in the canonical *ace* HDE_14279, producing G119S, A201S, F331Y, and L336M mutations. Despite the minimal within-gene level polymorphism, there was considerable among-gene level polymorphism (Figure 5). Across the 19 analyzed genes, there was an average of 7.1 variants (amino acids or deletions) at target-site codons, with a range of 3 to 13 variants. Particularly interesting was the observation that some *ace*-like genes in *H. destructor* were fixed for amino acids that are known to confer resistance in other arthropods (Feyereisen et al., 2015). Most striking were the following codons: codon 119, with 5/17 genes fixed for either A119 or S119 (Figure S1); codon 201, with 12/17 genes fixed for S201 (Figure S2); codon 227, with 8/18 genes fixed for A227 (Figure S3); codon 331, with 2/18 genes fixed for H331 (Figure S4); and codon 441, with 6/18 genes fixed for G441 (Figure S5). These unusual fixed alleles putatively conferring changes in amino acids that lead to resistance were found in both susceptible and resistant populations. Note that in some of the analyzed genes an equivalent target-site codon was absent, hence $n \neq 19$.

We found mixed support for the hypothesis that target-site mutations are associated with organophosphate insensitivity. If a mutation conferred insensitivity, we would expect that the differential in the mutant allele frequency (alive minus dead) would be positive. Yet this was not consistently the case. There were no significantly differentiated pairs of alive and dead mites for L331M in *ace*-like HDE_01555, R238K in *ace*-like HDE_01576, and L336M in canonical *ace* HDE_14279 (Figure 6a), which were found in both the resistant and susceptible populations. The G119S, A201S, and F331 mutations at canonical *ace* HDE_14279 were only observed in the resistant populations, as previously reported [29] (Figure 6a). Although there was evidence of some significant differentiation between alive and dead mites in resistant populations, the direction of the change was not consistent (Figure 6a).

The mixed patterns of differentiation in G119, A201S, and F331Y mutations in canonical *ace* are probably due to different haplotypes being selected by organophosphates. This was evidenced by negative correlations in the frequencies of target-site mutations (vs. the expected positive correlation if these mutations were linked) (Figure 6b). The A201S and F331Y mutations did not occur (or only rarely occurred) in the same resistant population: populations that were polymorphic for one of these mutant alleles were fixed (or almost fixed) for the wildtype at the other site (Figure 6b, right panel). In contrast, the G119S mutation was negatively correlated with A201S and (or) F331Y in some populations. For Colbinabbin Res, Tambellup, and Yongarillup, as the G119S mutant allele frequency increased, the A201S mutant allele frequency decreased (Figure 6b, left panel). For Manjimup, Treeton, and Yongarillup, as the G119S mutant allele frequency increased, the F331Y mutant allele frequency decreased (Figure 6b, middle panel). The apparent observable phases for resistant mutations based on allele frequencies appear to be: G119/S201, S119/A201, G119/Y331, S119/F331. However, the higher copy number at the canonical *ace* in Manjimup, Treeton, and Yongarillup complicates the picture; there may be haplotypes with different copy numbers segregating with different mutations in copies.

Genomic outlier scan

Two key results emerged from our genomic outlier scan: (1) signatures of selection were not discernible at the canonical *ace* or *ace*-like genes; and (2) there was no evidence of other enriched functions involved in

organophosphate insensitivity. On average, corrected block-wise F_{ST} between alive–dead sample pairs ranged from 0.008 to 0.035, with a mean of 0.0192, across the different populations (Figure S6). For Colbinabbin Res and Colbinabbin Sus, we had two independent untreated sample pairs that allowed us to assess the expected background corrected block-wise F_{ST}, which was 0.012 for both populations. This genetic differentiation between untreated samples was larger or equivalent to treated alive–dead sample pairs in both the Colbinabbin Res and Colbinabbin Sus populations. These results suggest that any genetic differentiation resulting from selection imposed by organophosphate exposure in our treated mites cannot be detected above a background of stochastic sampling noise in allele frequencies.

Across our samples pairs used in genomic outlier scans, in only one instance was an *ace*-like gene recovered (HDE_01553), but this was for an untreated sample pair (Colbinabbin Sus, sample 5 vs 4) where neither sample had been exposed to organophosphates. The genomic block containing the canonical *ace* was never significantly differentiated. A total of 474 unique genes were identified in outlier genomic blocks, but only 17 were shared by two populations. There was very little evidence for significant GO term enrichment in any alive–dead sample pair after accounting for multiple testing. Of those significant GO terms, 'Mannose metabolic process' and 'alpha-mannosidase activity' were enriched in the Colbinabbin Res 'treated 2' sample pair, and 'microtubule-based process' and 'dyein complex' were enriched in the Manjimup 'treated' sample pair. None of these GO terms have clear links to pesticide resistance.

Discussion

Our study suggests that a combination of copy number variation and target-site mutations may contribute to organophosphate insensitivity in Australian populations of *H. destructor*. Increased copy number can provide pesticide insensitivity through dosage effects (Kwon, Clarkt, & Lee, 2010; Deok Ho Kwon, Choi, Je, & Lee, 2012). At the canonical *ace* gene, we observed evidence of high mean copy number (≥2) in a subset of populations from Western Australia, which may help over-express target-site mutations (G119S, A201S, and F331Y) that are segregating at this gene. Such a mechanism has been observed in other arthropod pests, such as *Tetranychus evansi*, the tomato red spider mite [12] and the cotton aphid, *Aphis* gossyppii [47], and it is also common in organophosphate-resistant mosquito species [48].

Whilst the target-site mutations at the canonical *ace* are only segregating in resistant populations of *H. destructor*, they did not show clear patterns following organophosphate exposure. Indeed, even mites that were killed by organophosphates exhibited relatively high frequencies of G119S, A201S or F331Y at canonical *ace*. We were also unable to detect any signatures of selection at canonical *ace* from our genomic outlier scans. Multiple factors might have reduced our capacity to observe a clear signal in the canonical *ace* gene. First, the effect of the target-site mutations may not be large, which contrasts the pyrethroid resistance mechanism in *H. destructor* [27,28], and the clear effects of these same *ace* target-site mutations in other arthropod pests [5,12,49]. Second, target-site mutations could vary in their effects across different genetic backgrounds (Li et al., 2015; Riga et al., 2017). Third, haplotypes with different combinations of copy number and target-site mutations may vary in their effect sizes, such that organophosphates are not simply selecting for alleles at the canonical *ace*, but for different haplotypes. Long-read sequencing would be beneficial for resolving which haplotypes respond most to selection in *H. destructor*. We also suspect that the variation in the canonical *ace* is only one contributing component of a polygenic architecture of organophosphate insensitivity. Further genomic

investigations are required to discern the possible roles of detoxification (*e.g.,* cytochrome P450s, GSTs, esterases, or ABC transporters) or reduced penetrance (*e.g.,* cuticular proteins) mechanisms to organophosphate insensitivity in *H. destructor*.

The radiated *ace*-like genes may have more subtle contributions to organophosphate insensitivity. We have shown previously that these *ace*-like genes may be involved in complex haplotypes and structural variants, which may result in the presence or absence of different genes among individuals [29]. In this study, we provide further support for this hypothesis by demonstrating apparent copy numbers <1 for some *ace*-like genes. We also observed a significant association between copy number and organophosphate insensitivity, which suggests that surviving mites had slightly higher copies of (some) of these radiated *ace*-like genes. Amino acids at target-site positions were variable among *ace*-like genes. Duplication may relax evolutionary constraints on genes, allowing them to evolve more freely and accumulate mutations [52]. However, in some cases, we noticed a high proportion of known resistance-conferring mutations at these positions. The most striking was position 201, a major residue at the *ace* catalytic site, which forms part of the oxyanion hole [7]. At this site, the only alleles were either A201 (wild type) or S201 (mutant), for the canonical *ace* and all *ace*-like genes analysed; this is intriguing given the diversity observed at other sites and the known role of S201 in resistance. We note that the contribution of *ace*-like genes to organophosphate insensitivity are likely subtle: (i) estimated coefficients from our linear models were small; (ii) *ace*-like genes were not recovered from our genomic outlier scans; and (iii) radiated *ace*-like genes are found in organophosphate resistant and susceptible populations. We are currently exploring functional analyses to better understand how *ace*-like genes might contribute organophosphate insensitivity through possible sequestration or breakdown of pesticide molecules [30,31].

Given the accelerating spread of organophosphate resistance across Australian populations of *H. destructor* [21], clear diagnostic genetic markers of resistance would be highly advantageous [53]. At present, the canonical *ace* gene remains the strongest single candidate for developing molecular diagnostic of resistance risk in Australian populations of *H. destructor*. Our work points to variable ways in which the canonical *ace* and other *ace*-like genes in *H. destructor* may contribute to organophosphate insensitivity. The combination of canonical *ace* and radiated *ace*-like genes with other non-*ace* genes may allow populations of *H. destructor* to evolve diverse responses to organophosphate pesticides. The potential non-convergence and polygenicity of adaptation to organophosphates in *H. destructor* will need to be considered when using diagnostics of resistance in molecular monitoring programs.

Acknowledgements

This work was funded by the Grains Research Development Corporation (Australia) as part of the Australian Grains Pest Innovation Program, and with support from the University of Melbourne. Computational resources were provided by The University of Melbourne's Research Computing Services and the Petascale Campus Initiative. We thank our three anonymous reviewers for their comments, which greatly improved this manuscript.

Data accessibility

All sequencing data has been submitted under the GenBank Project PRJNA756307 and their accessions are listed in Table S1. All code and data required to run these analyses have been deposited into a Dryad archive [54]: https://doi.org/10.5061/dryad.dr7sqvb2m

Author contributions

JT formulated the original project design. PU and AH contributed to project design and obtained funding. JT performed all analyses. JT wrote the original manuscript. PU and AH contributed toward revisions of the final manuscript.

References

1 Davies TGE, Field LM, Usherwood PNR, and Williamson MS, DDT, pyrethrins, pyrethroids and insect sodium channels, *IUBMB Life* **59**:151–162 (2007).

2 Russell RJ, Claudianos C, Campbell PM, Horne I, Sutherland TD, and Oakeshott JG, Two major classes of target site insensitivity mutations confer resistance to organophosphate and carbamate insecticides, *Pestic Biochem Physiol* **79**:84–93 (2004).

3 Crossthwaite AJ, Rendine S, Stenta M, and Slater R, Target-site resistance to neonicotinoids, *J Chem Biol* **7**:125–128 (2014).

4 Foster SP, Harrington R, Devonshire AL, Denholm I, Devine GJ, Kenward MG, *et al.*, Comparative survival of insecticide-susceptible and resistant peach-potato aphids, *Myzus persicae* (Sulzer) (hemiptera: aphididae), in low temperature field trials, *Bull Entomol Res* **86**:17–27 (1996).

5 Khajehali J, van Leeuwen T, Grispou M, Morou E, Alout H, Weill M, *et al.*, Acetylcholinesterase point mutations in European strains of *Tetranychus urticae* (Acari: Tetranychidae) resistant to organophosphates, *Pest Manag Sci* **66**:220–228 (2010).

6 Martinez-Torres D, Devonshire AL, and Williamson MS, Molecular studies of knockdown resistance to pyrethroids: Cloning of domain II sodium channel gene sequences from insects, *Pestic Sci* **51**:265–270 (1997).

7 Oakeshott JG, Devonshire AL, Claudianos C, Sutherland TD, Horne I, Campbell PM, *et al.*, Comparing the organophosphorus and carbamate insecticide resistance mutations in cholin- and carboxyl-esterases, *Chem Biol Interact* **157**–**158**:269–275 (2005).

8 Fournier D, Mutations of acetylcholinesterase which confer insecticide resistance in insect populations, *Chem Biol Interact* **157**–**158**:257–261 (2005).

9 Feyereisen R, Dermauw W, and Van Leeuwen T, Genotype to phenotype, the molecular and physiological dimensions of resistance in arthropods, *Pestic Biochem Physiol* **121**:61–77 (2015).

10 Kwon DH, Choi JY, Je YH, and Lee SH, The overexpression of acetylcholinesterase compensates for the reduced catalytic activity caused by resistance-conferring mutations in *Tetranychus urticae*, *Insect Biochem Mol Biol* **42**:212–219, Elsevier Ltd (2012).

11 Kwon DH, Clarkt JM, and Lee SH, Extensive gene duplication of acetylcholinesterase associated with organophosphate resistance in the two-spotted spider mite, *Insect Mol Biol* **19**:195–204 (2010).

12 Carvalho R, Yang Y, Field LM, Gorman K, Moores G, Williamson MS, *et al.*, Chlorpyrifos resistance is associated with mutation and amplification of the acetylcholinesterase-1 gene in the tomato red spider mite, *Tetranychus evansi*, *Pestic Biochem Physiol* **104**:143–149, Elsevier Inc. (2012).

13 Langmüller AM, Nolte V, Galagedara R, Poupardin R, Dolezal M, and Schlötterer C, Fitness effects for *Ace* insecticide resistance mutations are determined by ambient temperature, *BMC Biol* **18**:1–11, BMC Biology (2020).

14 Freeman JC, San Miguel K, and Scott JG, All resistance alleles are not equal: the high fitness cost of super-kdr in the absence of insecticide, *Pest Manag Sci* **77**:3693–3697 (2021).

15 Crossley MS, Chen YH, Groves RL, and Schoville SD, Landscape genomics of Colorado potato beetle provides evidence of polygenic adaptation to insecticides, *Mol Ecol*:6284–6300 (2017).

16 Devonshire AL and Moores GD, A carboxylesterase with broad substrate specificity causes organophosphorus, carbamate and pyrethroid resistance in peach-potato aphids (*Myzus persicae*), *Pestic Biochem Physiol* **18**:235–246 (1982).

17 Walsh TK, Joussen N, Tian K, Mcgaughran A, Anderson CJ, Qiu X, *et al.*, Multiple recombination events between two cytochrome P450 loci contribute to global pyrethroid resistance in *Helicoverpa armigera*, *PLoS One* **13**:e0197760 (2018).

18 Hsu JC, Lin YY, Chang CC, Hua KH, May Chen MJ, Huang LH, *et al.*, Discovery of organophosphate resistance-related genes associated with well-known resistance mechanisms of *Plutella xylostella* (L.) (Lepidoptera: Plutellidae) by RNA-Seq, *J Econ Entomol* **109**:1378–1386 (2016).

19 Newman LJ, The red legged earth mite *Penthaleus destructor* (Jack), *J Dep Agric West Aust* **2**:469–475 (1925).

20 Ridsdill-Smith TJ, Biology and control of *Halotydeus destructor* (Tucker) (Acarina: Penthaleidae): A review, *Exp Appl Acarol* **21**:195–224 (1997).

21 Arthur AL, Maino J, Hoffmann AA, Jasper M, Lord A, Micic S, *et al.*, Learnings from over a decade of increasing pesticide resistance in the redlegged earth mite, *Halotydeus destructor* (Tucker), *Pest Manag Sci* **77**:3013–3024 (2021).

22 Umina PA, McDonald G, Maino J, Edwards O, and Hoffmann AA, Escalating insecticide resistance in Australian grain pests: contributing factors, industry trends and management opportunities, *Pest Manag Sci* **75**:1494–1506 (2019).

23 Hoffmann AA, Porter S, and Kovacs I, The response of the major crop and pasture pest, the red-legged earth mite (*Halotydeus destructor*) to pesticides: Dose-response curves and evidence for tolerance, *Exp Appl Acarol* **21**:151–162 (1997).

24 Robinson MT and Hoffmann AA, Additional tests on the effects of pesticides on cryptic species of blue oat mite (*Penthaleus* spp.) and the redlegged earth mite (*Halotydeus destructor*), *Aust J Exp Agric* **40**:671–678 (2000).

25 Umina PA, Pyrethroid resistance discovered in a major agricultural pest in southern Australia: the redlegged earth mite *Halotydeus destructor* (Acari: Penthaleidae), *Pest Manag Sci* **63**:1185–1190 (2007).

26 Cheng X, Umina PA, Lee SF, and Hoffmann AA, Pyrethroid resistance in the pest mite, *Halotydeus destructor*: Dominance patterns and a new method for resistance screening, *Pestic Biochem Physiol* **159**:9–16 (2019).

27 Edwards OR, Walsh TK, Metcalfe S, Tay WT, Hoffmann AA, Mangano P, *et al.*, A genomic approach to identify and monitor a novel pyrethroid resistance mutation in the redlegged earth mite, *Halotydeus destructor*, *Pestic Biochem Physiol* **144**:83–90 (2018).

28 Yang Q, Umina PA, Rašić G, Bell N, Fang J, Lord A, *et al.*, Origin of resistance to pyrethroids in the redlegged earth mite (*Halotydeus destructor*) in Australia: repeated local evolution and migration, *Pest Manag Sci* (2020).

29 Thia JA, Korhonen PK, Young ND, Gasser RB, Umina PA, Yang Q, *et al.*, The redlegged earth mite draft genome provides new insights into pesticide resistance evolution and demography in its invasive Australian range, *J Evol Biol* **36**:381–398 (2023).

30 Kim YH, Cha DJ, Jung JW, Kwon HW, and Lee SH, Molecular and Kinetic Properties of Two Acetylcholinesterases from the Western Honey Bee, Apis mellifera, *PLoS One* **7**:17–19 (2012).

31 Newcomb RD, Campbell PM, Ollis DL, Cheah E, Russell RJ, and Oakeshott JG, A single amino acid substitution converts a carboxylesterase to an organophosphorus hydrolase and confers insecticide resistance on a blowfly, *PNAS* **94**:7464–7468 (1997).

32 Chen S, Zhou Y, Chen Y, and Gu J, fastp: an ultra-fast all-in-one FASTQ preprocessor, *Bioinformatics* **34**:i884–i890 (2018).

33 Langmead B and Salzberg SL, Fast gapped-read alignment with Bowtie 2, *Nat Methods* **9**:357–359 (2012).

34 Danecek P, Bonfield JK, Liddle J, Marshall J, Ohan V, Pollard MO, *et al.*, Twelve years of SAMtools and BCFtools, *Gigascience* **10**:giab008, Oxford University Press (2021).

35 Li H, Handsaker B, Wysoker A, Fennell T, Ruan J, Homer N, *et al.*, The sequence alignment/map format and SAMtools, *Bioinformatics* **25**:2078–2079 (2009).

36 Garrison E and Marth G, Haplotype-based variant detection from short-read sequencing, *arXiv* **1207.3907** (2012).

37 Li H, A statistical framework for SNP calling, mutation discovery, association mapping and population genetical parameter estimation from sequencing data, *Bioinformatics* **27**:2987–2993, Oxford University Press (2011).

38 Danecek P, Auton A, Abecasis G, Albers CA, Banks E, DePristo MA, *et al.*, The variant call format and VCFtools, *Bioinformatics* **27**:2156–2158 (2011).

39 R Core Team, R: A language and environment for statistical computing (v4.1.3) (2022).

40 Bates D, Mächler M, Bolker B, and Walker S, Fitting linear mixed-effects models using lme4, *arXiv Prepr* (2014).

41 Kuznetsova A, Brockhoff PB, and Christensen RHB, lmerTest package: tests in linear mixed effects models, *J Stat Softw* **82**:1–26 (2017).

42 Lawrence M, Huber W, Pages H, Aboyoun P, Carlson M, Gentleman R, *et al.*, Software for computing and

annotating genomic ranges, *PLOS Comput Biol Biol* **9**:e1003118, Public Library of Science San Francisco, USA (2013).

43 Pagès H, Aboyoun P, Gentleman R, and DebRoy S, Biostrings: Efficient manipulation of biological strings, *R Packag* (2017).

44 Weir BS and Cockerham CC, Estimating F-statistics for the analysis of population structure, *Evolution (N Y)* **38**:1358–1370 (1984).

45 Whitlock MC and Lotterhos KE, Reliable Detection of Loci Responsible for Local Adaptation: Inference of a Null Model through Trimming the Distribution of F_{ST}, *Am Nat* **186**:S24–S36 (2015).

46 Whitlock MC, OutFLANK: A procedure to find Fst outliers based on an inferred distribution of neutral Fst (2019).

47 Shang Q, Pan Y, Fang K, Xi J, Wong A, Brennan JA, *et al.*, Extensive *Ace2* duplication and multiple mutations on *Ace1* and *Ace2* are related with high level of organophosphates resistance in *Aphis gossypii*, *Environ Toxicol* **29**:526–533 (2014).

48 Weetman D, Djogbenou LS, and Lucas E, Copy number variation (CNV) and insecticide resistance in mosquitoes: evolving knowledge or an evolving problem?, *Curr Opin Insect Sci* **27**:82–88, Elsevier Inc. (2018).

49 Andrews M, Callaghan A, Field L, Williamson M, and Moores G, Identification of mutations conferring insecticide-insensitive AChE in the cotton-melon aphid, *Aphis gossypii* Glover, 555–561 (2004).

50 Li CX, Kaufman PE, Xue R De, Zhao MH, Wang G, Yan T, *et al.*, Relationship between insecticide resistance and kdr mutations in the dengue vector *Aedes aegypti* in Southern China, *Parasites and Vectors* **8**:1–9, Parasites & Vectors (2015).

51 Riga M, Bajda S, Themistokleous C, Papadaki S, Palzewicz M, Dermauw W, *et al.*, The relative contribution of target-site mutations in complex acaricide resistant phenotypes as assessed by marker assisted backcrossing in Tetranychus urticae, *Sci Rep* **7**:1–12 (2017).

52 Lynch M and Conery JS, The evolutionary fate and consequences of duplicate genes, *Science (80-)* **290**:1151–1155, American Association for the Advancement of Science (2000).

53 Thia JA, Hoffmann AA, and Umina PA, Empowering Australian insecticide resistance research with genetic information: the road ahead, *Austral Entomol* **60**:147–162 (2021).

54 Thia JA, Dataset for “Evolution of an acetylcholinesterase gene complex and its contribution toward organophosphate insensitivity in an invasive mite pest” (2022).

Tables and figures

Table 1. Sample contrasts for testing genetic differences between pooled *H. destructor* samples that were untreated (stochastic background differences) or treated (potential selected differences) with organophosphate.

Sample 1	Sample 2	Code	Population	Contrast
2	3	ColS: untreated	Colbinabbin Sus	Untreated
4	5	ColR: untreated	Colbinabbin Res	Untreated
6	8	ColS: treated 1	Colbinabbin Sus	Treated
7	9	ColS: treated 2	Colbinabbin Sus	Treated
10	12	ColR: treated 1	Colbinabbin Res	Treated
11	13	ColR: treated 2	Colbinabbin Res	Treated
18	19	Tamb: treated	Tambellup	Treated
20	21	Tree: treated	Treeton	Treated
26|28	27|29	Yong: treated	Yongarillup	Treated
38|39	40|41	Manj: treated	Manjimup	Treated

Table 2. Single Nucleotide Polymorphisms (SNPs) within candidate *ace* target-site codons and their effects on coding potential in *H. destructor*. The ancestral *ace* gene (HDE_14279) is bolded.

Tcal	Hdes	*Ace* gene ID number	Contig	Position	Ref allele	Alt allele	Non-synonymous
78	86	HDE_01576	utg155	546035	V (GTA)	V (GTG)	.
119	129	HDE_09762	utg48	258743	G (GGG)	G (GGA)	.
	191	**HDE_14279**	**utg94**	**20925**	**G (GGC)**	**S (AGC)**	**Yes**
128	277	HDE_13905	utg83	1999982	E (GAG)	E (GAA)	.
150	159	HDE_01556	utg155	503437	P (CCC)	P (CCA)	.
201	210	HDE_01553	utg155	499445	S (TCG)	S (TCT)	.
	207	HDE_05340	utg31	94639	S (TCA)	S (TCG)	.
201	**272**	**HDE_14279**	**utg94**	**21168**	**A (GCC)**	**S (TCC)**	**Yes**
227	337	HDE_01190	utg153	521028	G (GGC)	G (GGA)	.
	5	HDE_01555	utg155	501653	A (GCG)	A (GCA)	.
227	238	HDE_02989	utg19	1187910	G (GGA)	G (GGC)	.
238	241	HDE_01576	utg155	546499	R (AGG)	K (AAG)	Yes
331	97	HDE_01555	utg155	501929	L (CTC)	M (CTG)	Yes
	326	HDE_01576	utg155	546755	H (CAC)	H (CAT)	.
	401	**HDE_14279**	**utg94**	**21556**	**F (TTC)**	**Y (TAC)**	**Yes**
336	450	HDE_01190	utg153	521367	F (TTT)	F (TTC)	.
	406	**HDE_14279**	**utg94**	**21572**	**L (CTA)**	**M (CTG)**	**Yes**
396	544	HDE_07881	utg40	396829	G (GGC)	G (GGT)	.
441	589	HDE_07881	utg40	396694	G (GGC)	G (GGA)	.

Note: Codons are reported with respect to their candidate *ace* position in *T. californica* ('Tcal') and their relative *H. destructor* codon ('Hdes'). Alleles are reported with respect to their amino acid residue, with nucleotide bases comprising the codon in brackets.

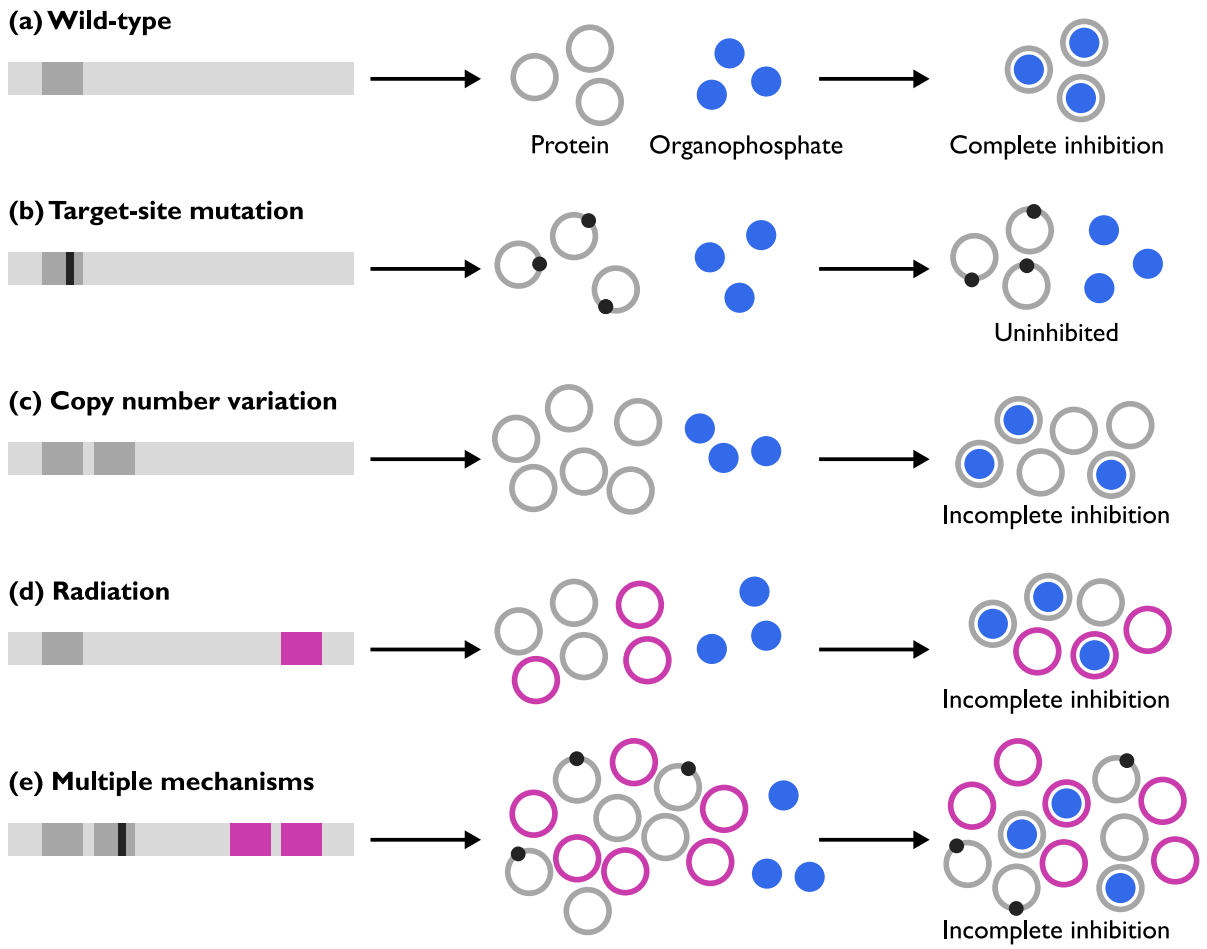

Figure 1. Schematic of hypothesized mechanisms for canonical *ace* and radiated *ace*-like genes to organophosphate insensitivity. All mechanisms reduce inhibition of the canonical *ace*. (a) The wild-type canonical *ace* gene produces protein that is sensitive to organophosphate inhibition. (b) Target-site mutations in the canonical *ace* gene allow production of protein that is insensitive to organophosphate inhibition. (c) Increasing copy number of the canonical *ace* helps over-express the protein product, requiring more organophosphate molecules to achieve complete inhibition. (d) Radiated *ace* genes help sequester or breakdown organophosphate pesticides, reducing inhibition of canonical *ace* proteins. (e) Multiple mechanisms combine to reduce inhibition of the canonical *ace* proteins.

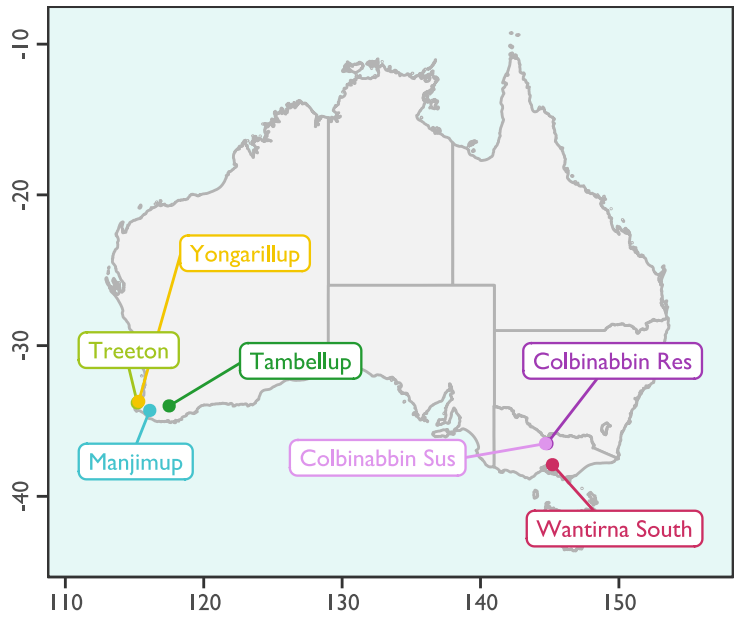

Figure 2. Map of Australia illustrating the locations of our studied populations

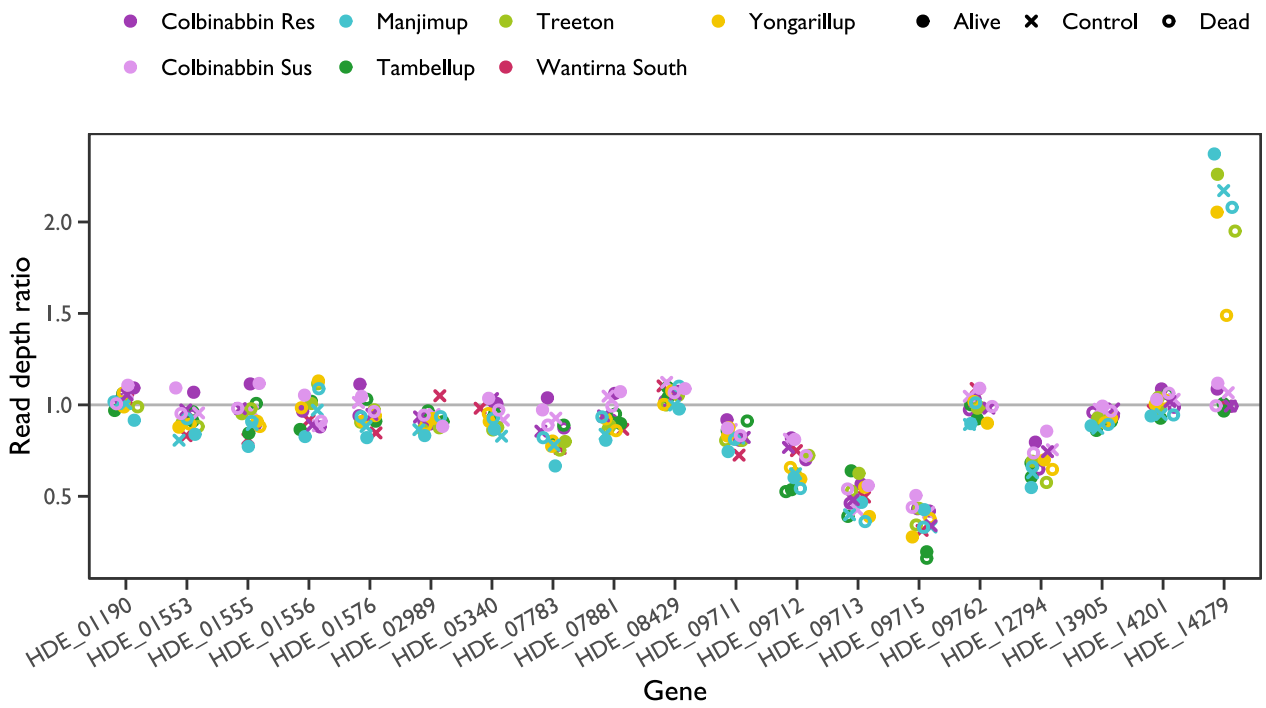

Figure 3. Mean copy number at the canonical ace and *ace*-like genes in population pool-seq samples of *H. destructor*. The *x*-axis represents the 18 focal ace-like genes and the canonical *ace* (HDE_14279). The *y*-axis represents the mean read depth ratio (a proxy for copy number), which is the read depth of the canonical or *ace*-like gene divided by the read depth of 866 single copy reference genes. Points represent samples: colors and shapes denote population and survival status (see legend). The grey horizontal line demarcates a read depth ratio (copy number) of one.

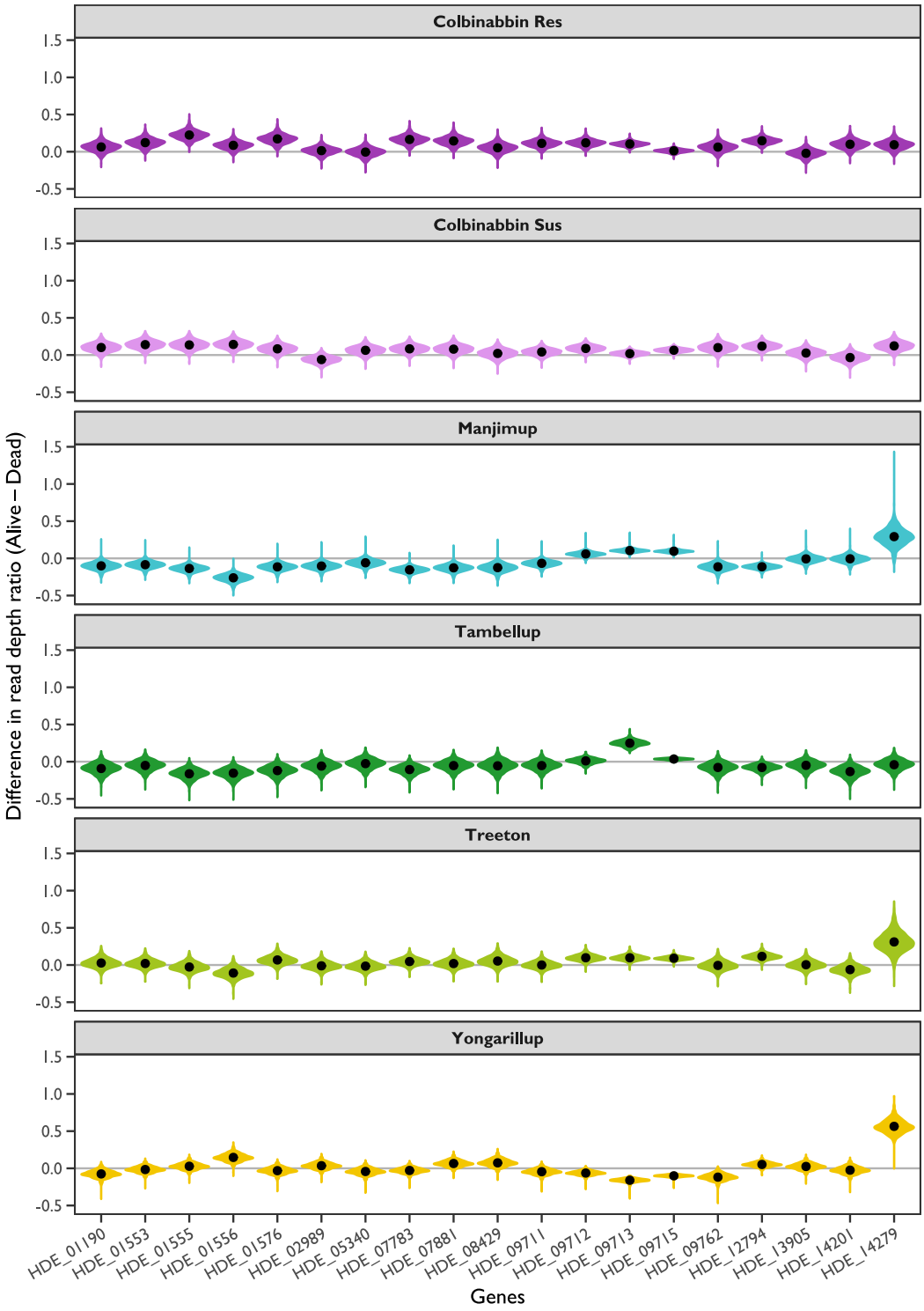

Figure 4. Differences in canonical *ace* or *ace*-like gene copy number between alive and death mites following organophosphate exposure. The *x*-axis represents the 18 focal ace-like genes and the canonical *ace* (HDE_14279). The *y*-axis represents the difference in gene copy number as estimated by the read depth ratio between alive and dead mites (alive – dead). Black points represent the mean difference relative to estimates from 866 single copy reference genes. Violin plots summarise the distribution of estimates. The grey line demarcates a difference of zero. Each panel represents a population.

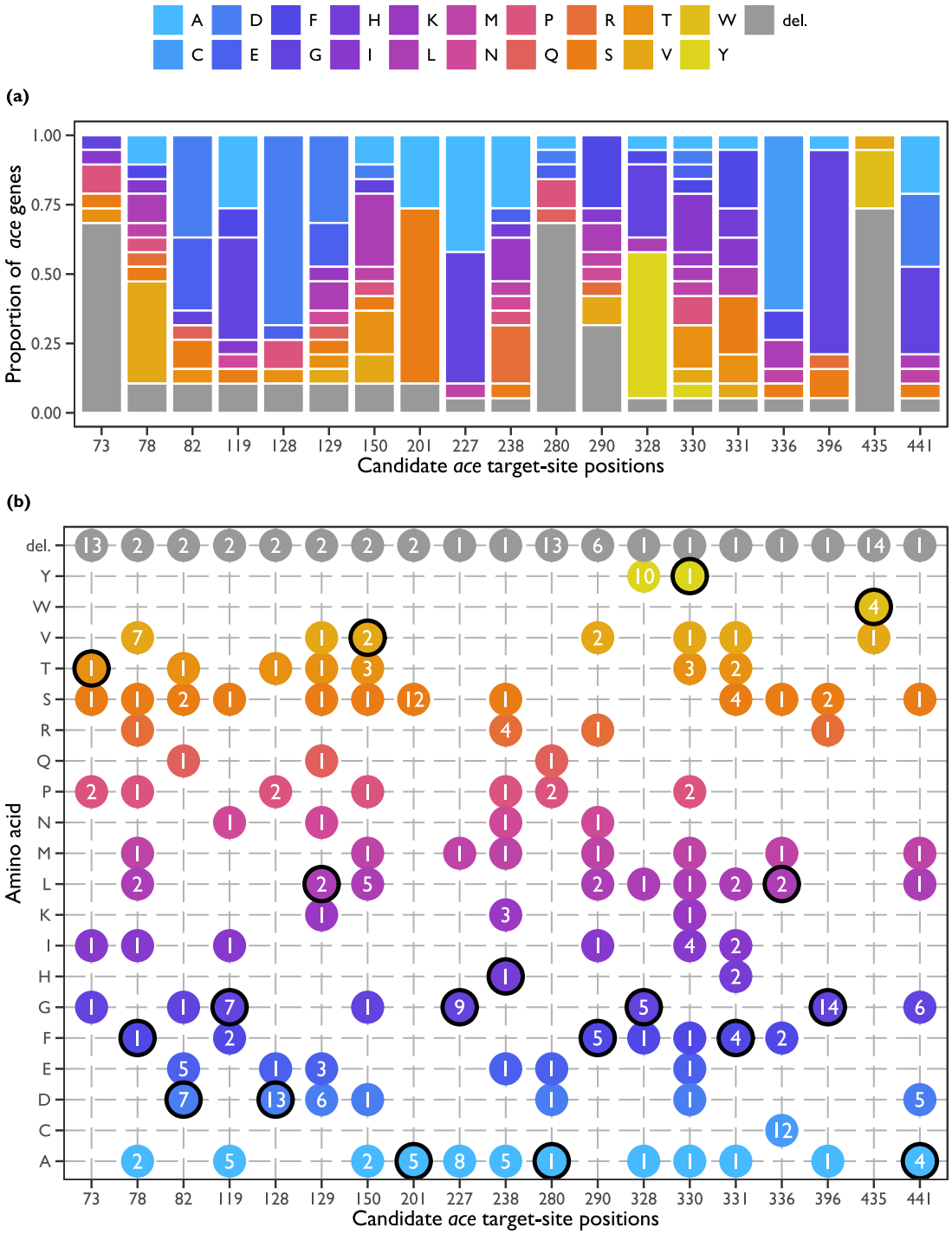

Figure 5. Reference amino acids across the *H. destructor* canonical *ace* and focal 18 *ace*-like genes (on contigs >0.2 Mb) at candidate target-site codons (*T. californica* numbering). (a) Amino acid proportions. The *x*-axis is the candidate *ace* target-site codon, the *y*-axis is the relative proportion of *ace* genes exhibiting a particular amino acid as their reference allele (see legend) in the *H. destructor* genome. (b) Amino acid counts. The *x*-axis is the candidate *ace* target-site codon, the *y*-axis is the *ace* gene numbers exhibiting a particular amino acid as their reference allele in the *H. destructor* genome. A black outline denotes the amino acid present in the canonical *ace* gene, HDE_14279. (a, b) 'del.' indicates a deletion, that is, where there is no equivalent codon in the *H. destructor* gene relative to *T. californica*.

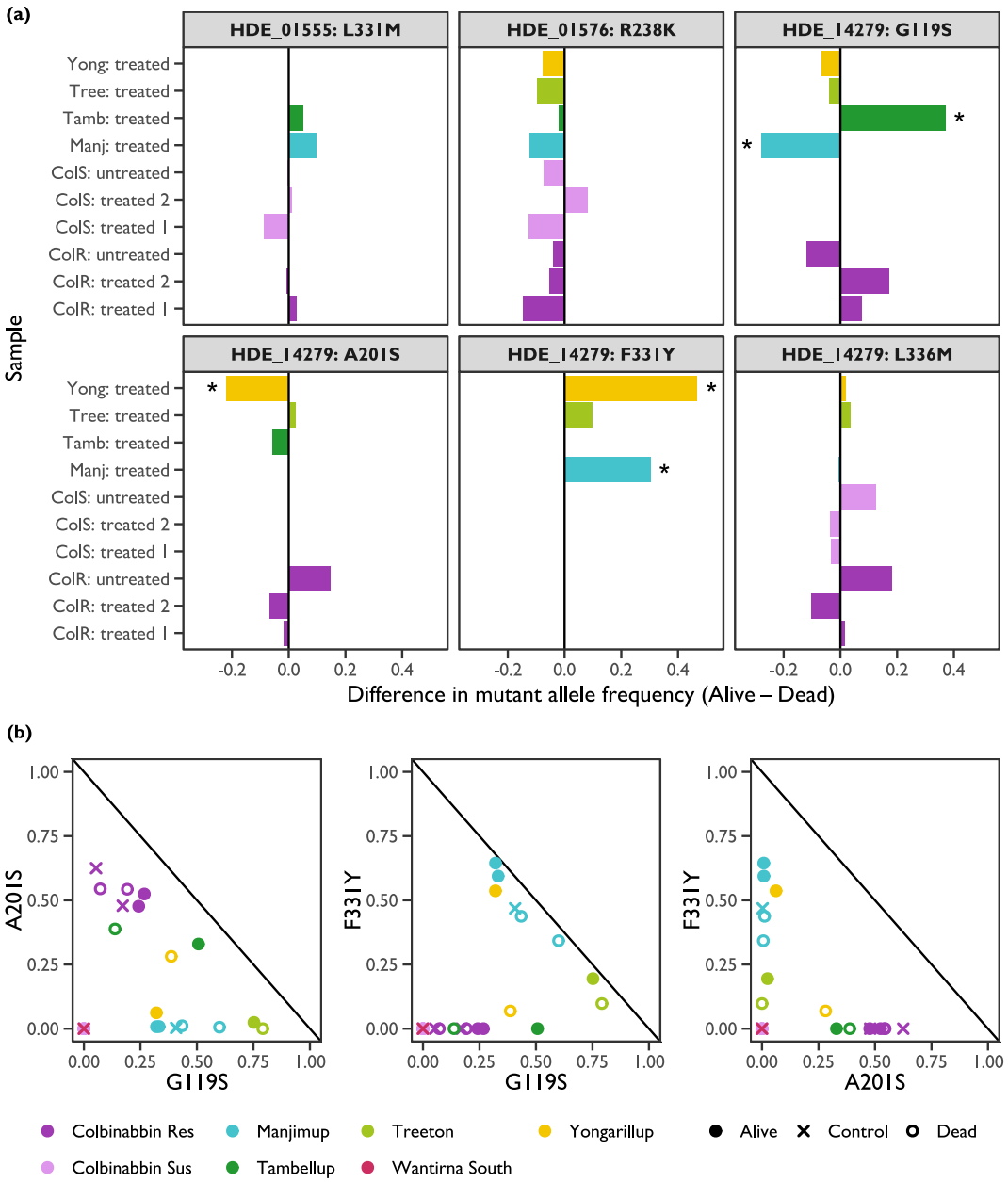

Figure 6. Allelic variation for non-synonymous mutations at candidate *ace* target-sites codons in *H. destructor* (with *Torpedo californica* numbering). (a) Mutant allele frequency difference between alive and dead exposed to organophosphates ('treated') or between two unexposed samples ('untreated). Bars on the *x*-axis represents the allele frequency difference and populations are organized on the *y*-axis. Positive values on the *x*-axis indicate samples of alive mites had a higher mutation allele frequency relative to samples of dead mites. Asterisks denote significant allele count differences following Bonferroni correction for multiple tests (χ^2 test, α = 0.05/50 = 0.001). Population codes are: 'ColR' = Colbinabbin Res, 'ColS' = Colbinabbin Sus, 'Manj' = Manjimup, 'Tamb' = Tambellup, 'Tree' = Treeton, and 'Yong' = Yongarillup. Each panel represents a gene and mutation; note that the canonical *ace* gene is HDE_14279. (b) Mutant allele frequency correlations for target-site mutations at the canonical *ace* gene, HDE_14279. The *x*-axis and *y*-axis represent the frequencies of one of three target-site mutations. The 1:1 negative correlation is depicted by the black line. Symbols represent samples, with colours denoting population, and shapes denoting survival group (see legend).

Supplementary information

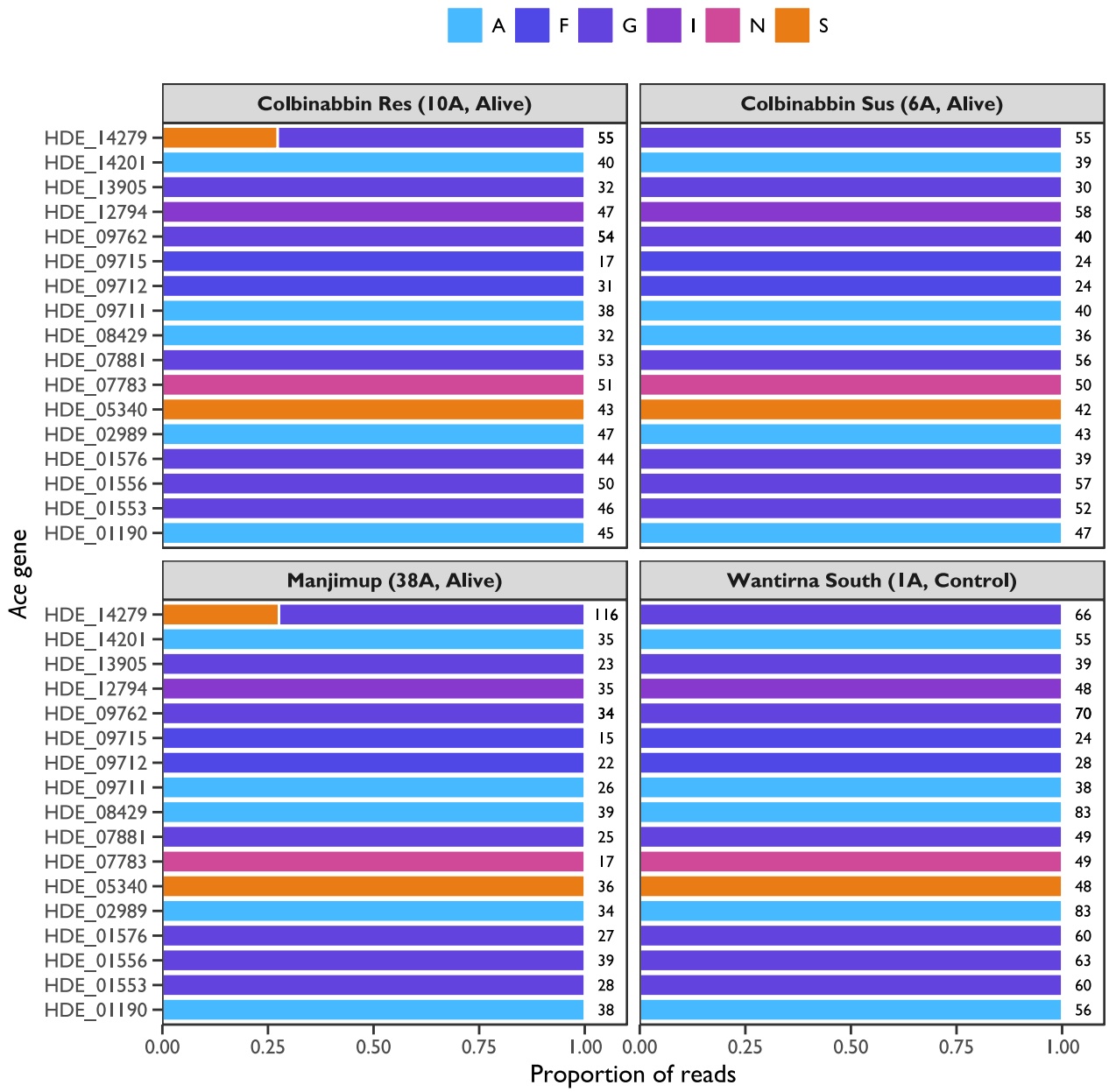

Figure S1. Proportion of reads for different amino acids at codon 119 (*Torpedo californica* numbering) across *ace* genes in *Halotydeus destructor*. The *x*-axis is the proportion of reads and the *y*-axis the *ace* gene. Horizontal bars represent the proportion of reads with nucleotide sequences encoding different amino acids, see legend. Numbers to the right of the bars indicate the number of observed reads that completely covered the codon. Panels contain observations for select pool-seq libraries, read as 'Population (DNA pool, Survival group)'. Note, Colbinabbin Res and Manjimup are resistant to organophosphates, whereas Colbinabbin Sus and Wantirna South are susceptible.

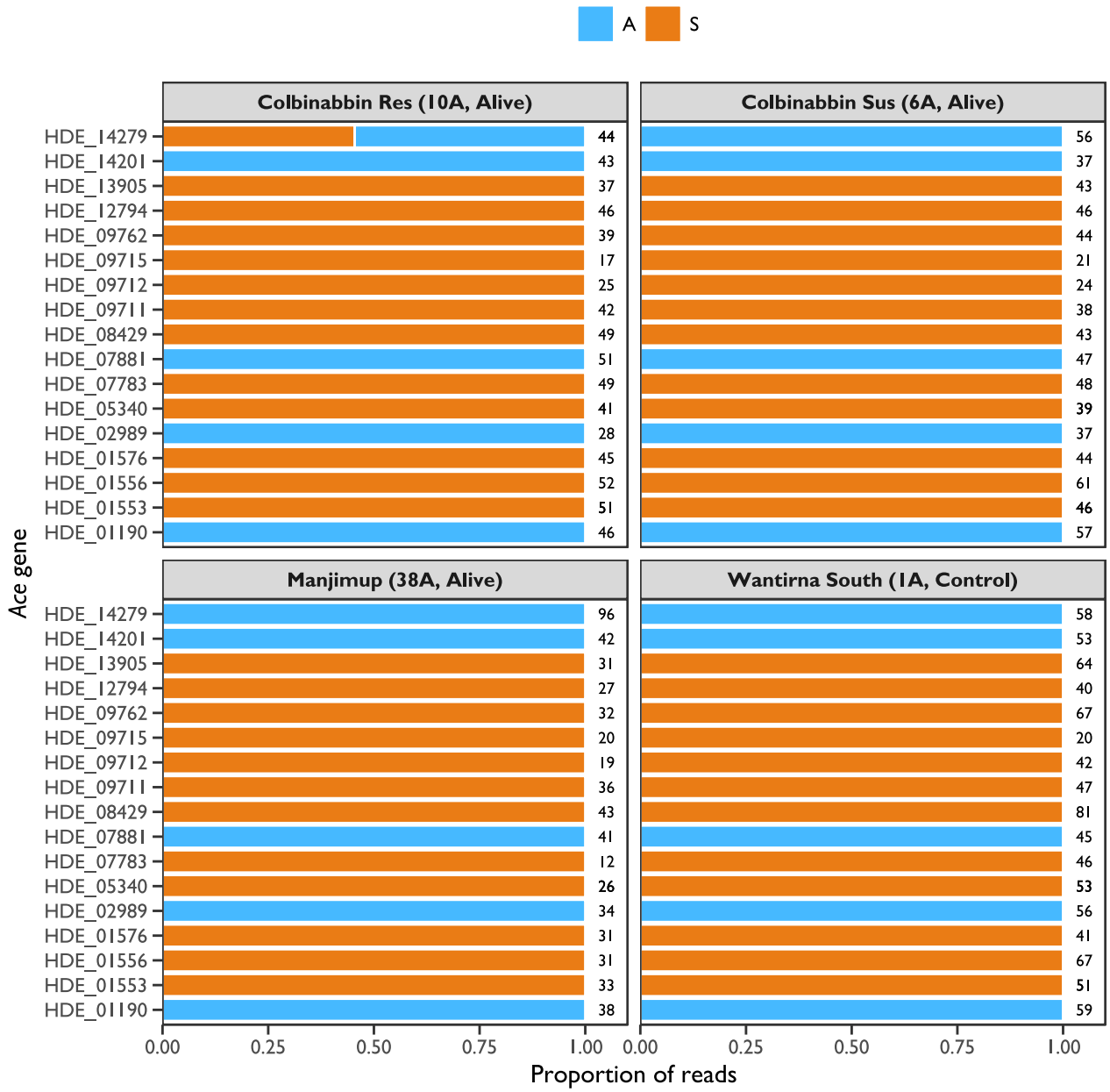

Figure S2. Proportion of reads for different amino acids at codon 201 (*Torpedo californica* numbering) across *ace* genes in *Halotydeus destructor*. The *x*-axis is the proportion of reads and the *y*-axis the *ace* gene. Horizontal bars represent the proportion of reads with nucleotide sequences encoding different amino acids, see legend. Numbers to the right of the bars indicate the number of observed reads that completely covered the codon. Panels contain observations for select pool-seq libraries, read as 'Population (DNA pool, Survival group)'. Note, Colbinabbin Res and Manjimup are resistant to organophosphates, whereas Colbinabbin Sus and Wantirna South are susceptible.

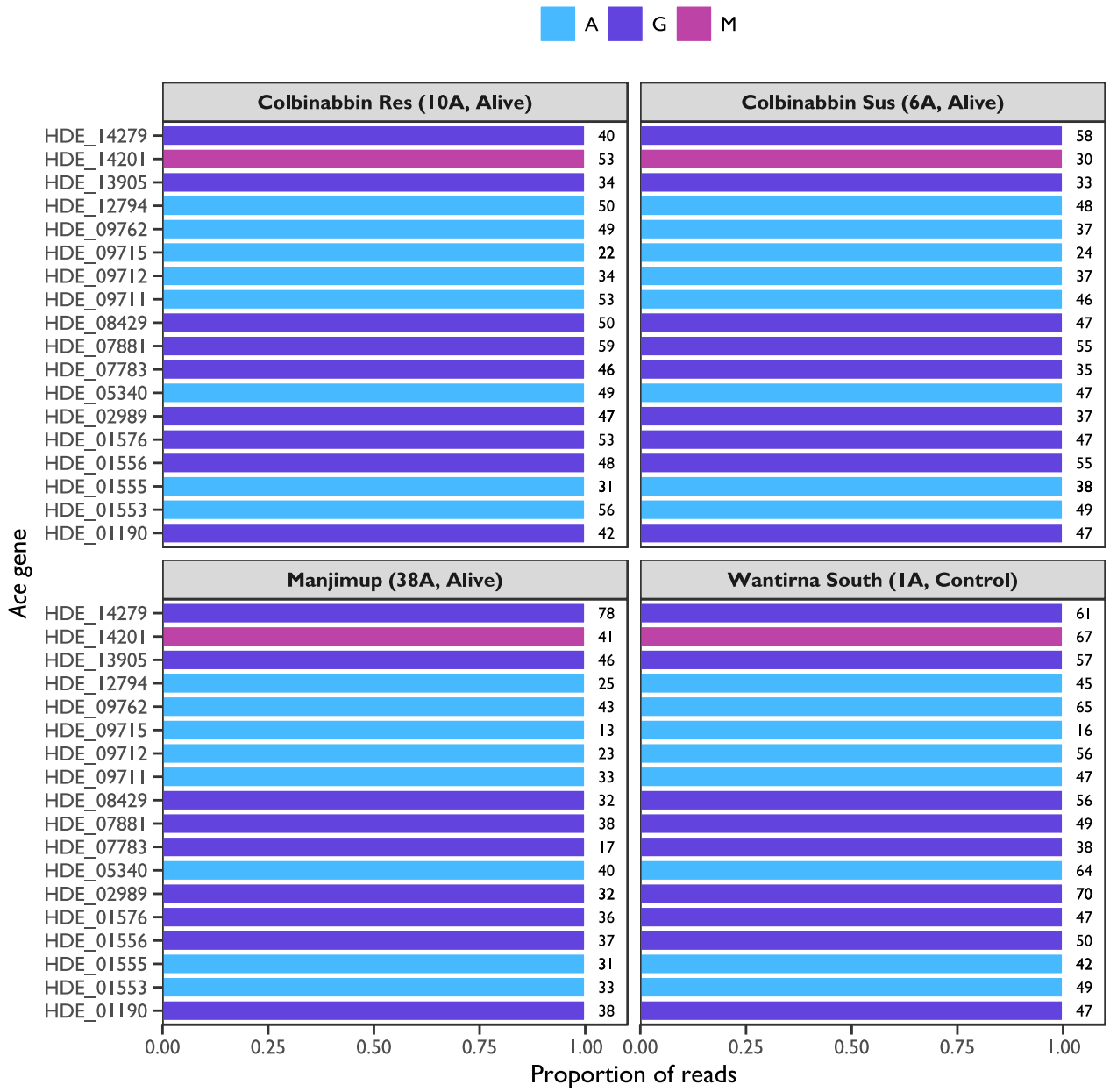

Figure S3. Proportion of reads for different amino acids at codon 227 (*Torpedo californica* numbering) across *ace* genes in *Halotydeus destructor*. The *x*-axis is the proportion of reads and the *y*-axis the *ace* gene. Horizontal bars represent the proportion of reads with nucleotide sequences encoding different amino acids, see legend. Numbers to the right of the bars indicate the number of observed reads that completely covered the codon. Panels contain observations for select pool-seq libraries, read as 'Population (DNA pool, Survival group)'. Note, Colbinabbin Res and Manjimup are resistant to organophosphates, whereas Colbinabbin Sus and Wantirna South are susceptible.

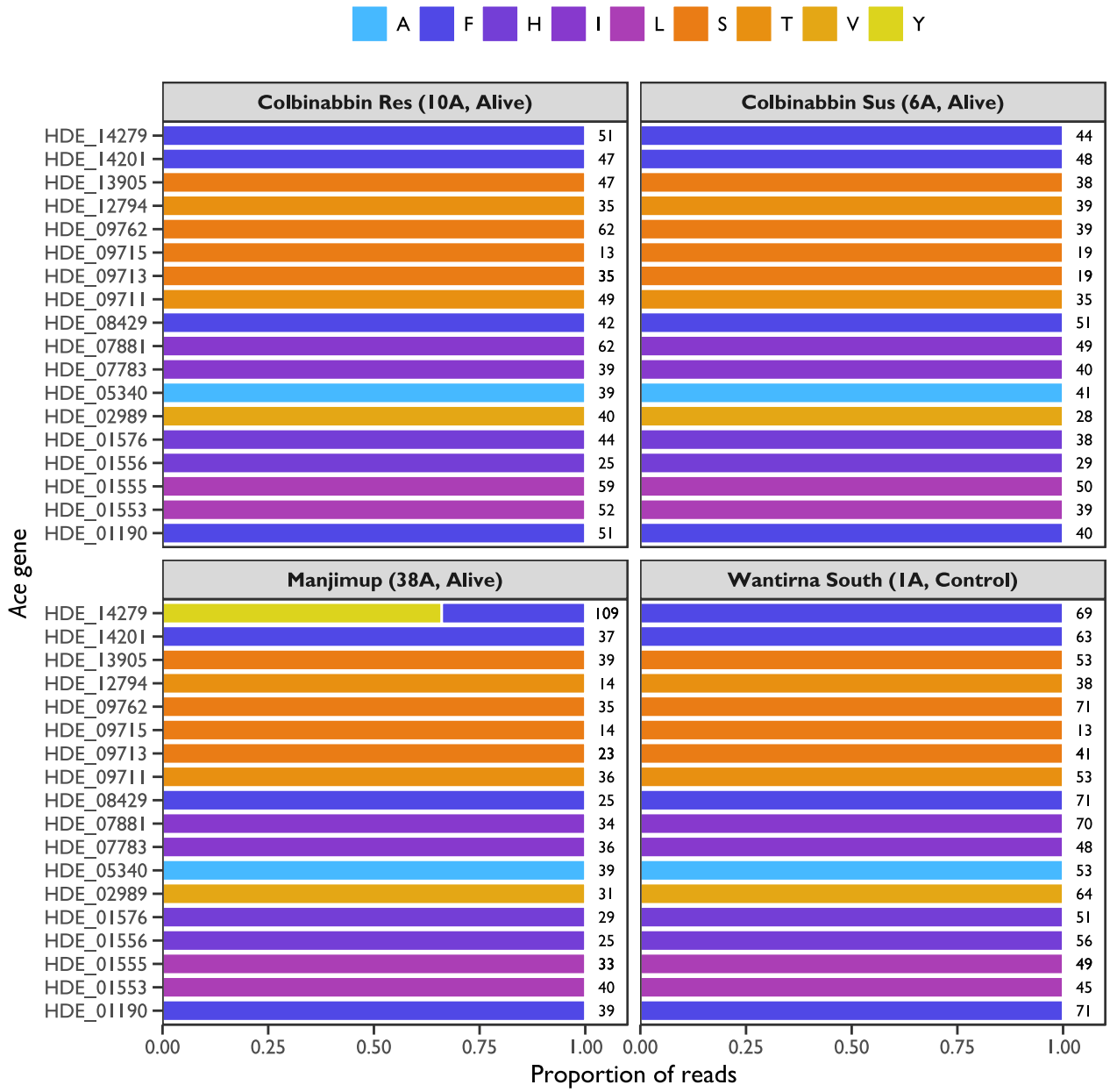

Figure S4. Proportion of reads for different amino acids at codon 331 (*Torpedo californica* numbering) across *ace* genes in *Halotydeus destructor*. The *x*-axis is the proportion of reads and the *y*-axis the *ace* gene. Horizontal bars represent the proportion of reads with nucleotide sequences encoding different amino acids, see legend. Numbers to the right of the bars indicate the number of observed reads that completely covered the codon. Panels contain observations for select pool-seq libraries, read as 'Population (DNA pool, Survival group)'. Note, Colbinabbin Res and Manjimup are resistant to organophosphates, whereas Colbinabbin Sus and Wantirna South are susceptible.

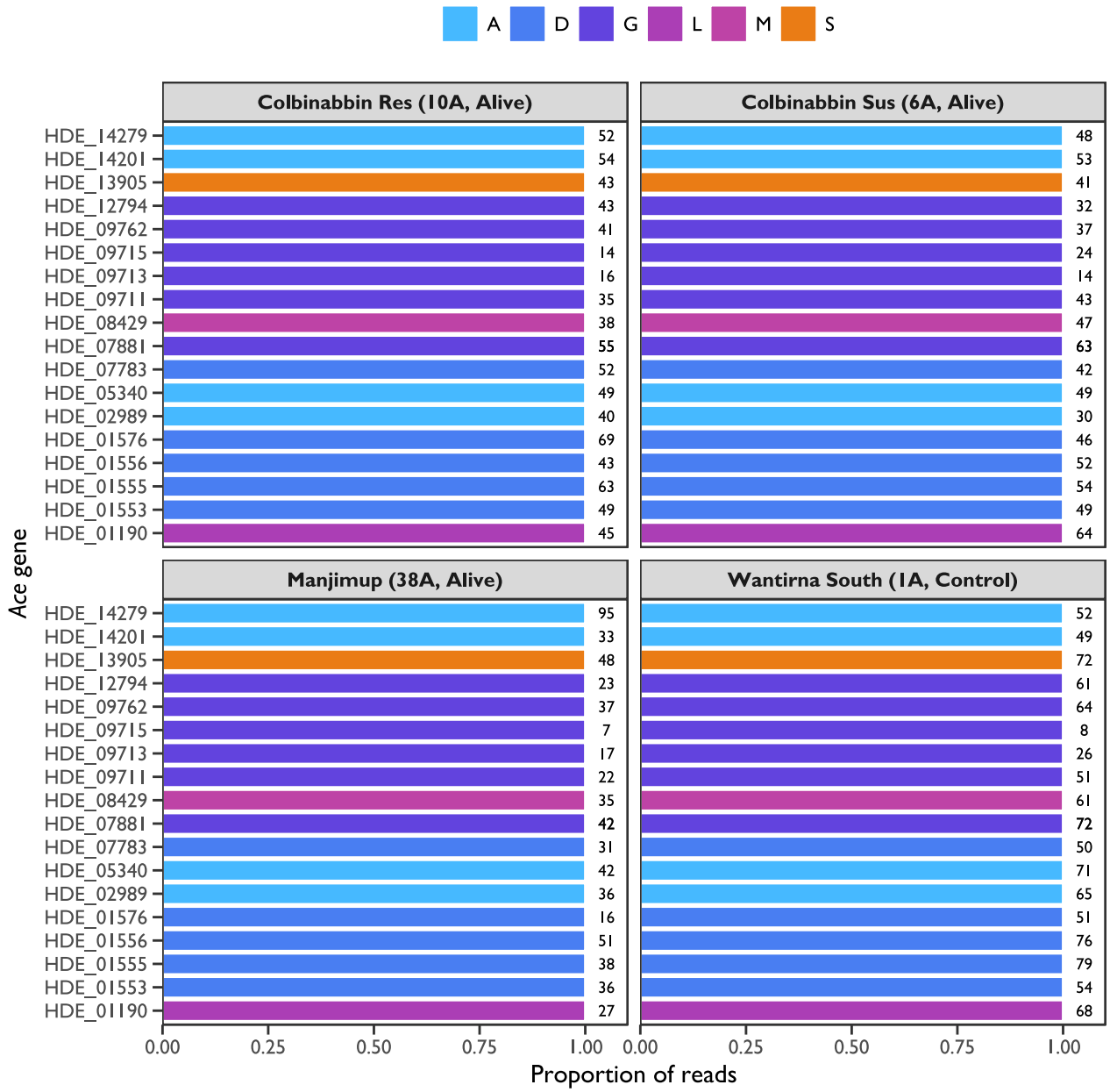

Figure S5. Proportion of reads for different amino acids at codon 441 (*Torpedo californica* numbering) across *ace* genes in *Halotydeus destructor*. The *x*-axis is the proportion of reads and the *y*-axis the *ace* gene. Horizontal bars represent the proportion of reads with nucleotide sequences encoding different amino acids, see legend. Numbers to the right of the bars indicate the number of observed reads that completely covered the codon. Panels contain observations for select pool-seq libraries, read as 'Population (DNA pool, Survival group)'. Note, Colbinabbin Res and Manjimup are resistant to organophosphates, whereas Colbinabbin Sus and Wantirna South are susceptible.

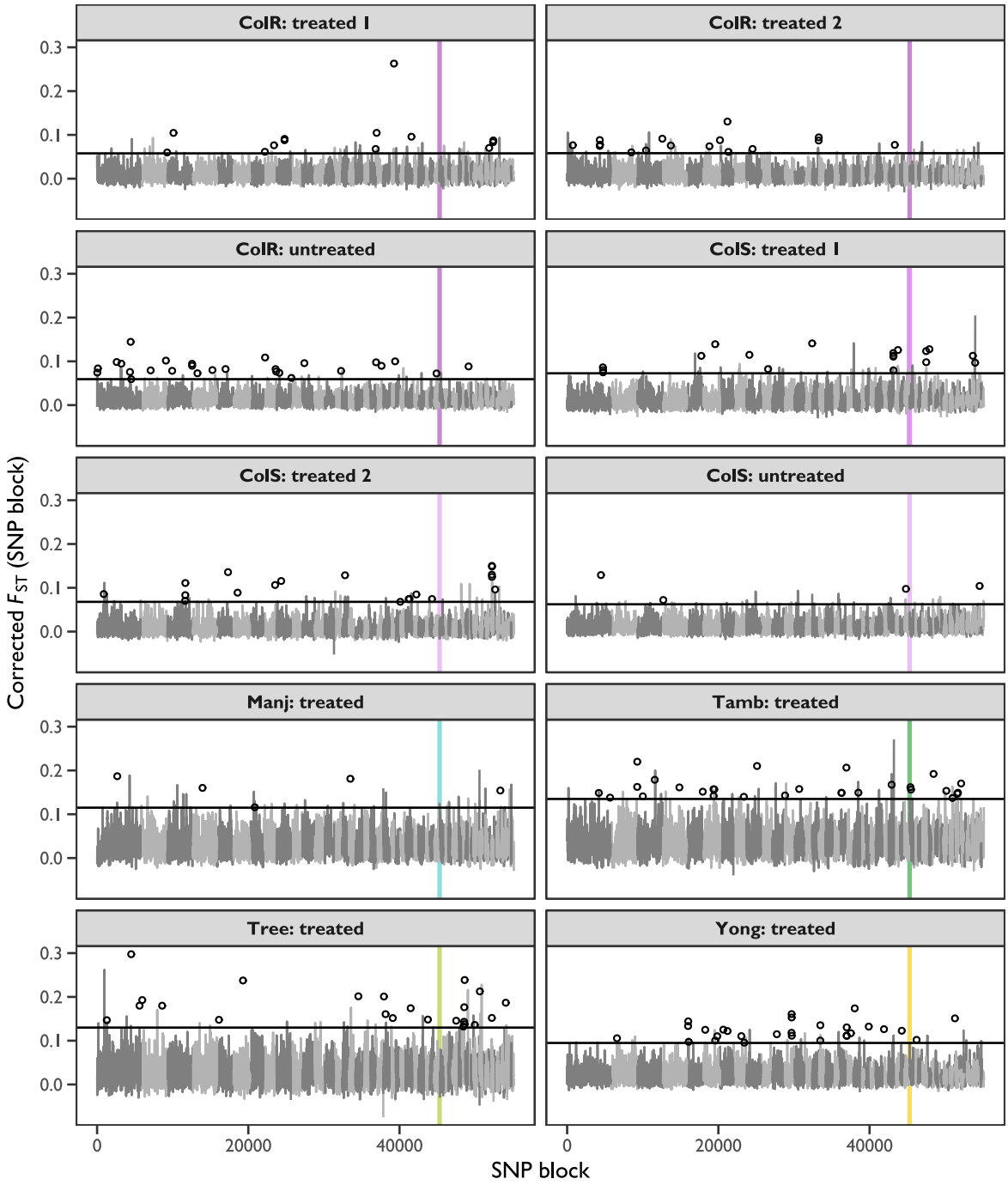

Figure S6. Genome outlier scans between alive and dead samples of *H. destructor* following organophosphate exposure. The *x*-axis represents the SNP block, indexed by contig size and linear order. The *y*-axis is the F_{ST} corrected for sampling variance. Black horizontal lines demarcate the 99th percentile of F_{ST}. Grey lines track the F_{ST} of *non-outlier* SNP blocks, with alternating shades of grey delimiting separate contigs. Open points denote *outlier* SNP blocks. Coloured vertical lines indicate SNP blocks containing the canonical *ace* gene. Panels contain different sample contrasts (see Table 1). Population codes are as follows: 'ColR' = Colbinabbin Res, 'ColS' = Colbinabbin Sus, 'Manj' = Manjimup, 'Tamb' = Tambellup, 'Tree' = Treeton, and 'Yong' = Yongarillup. Sample contrasts include 'untreated', which is the F_{ST} between two samples *unexposed* to organophosphate, and 'treated', which is the F_{ST} between samples of alive and dead mites that were *exposed* to organophosphate.

Table S1. Metadata for pool-seq libraries. All *H. destructor* libraries were nested in DNA pools nested in biological samples (NCBI SRA and BioSample accession numbers listed for each library).

Sample	Pool	Library	Population	No. diploid individuals	Pesticide	Pesticide dose (mg/L)	Survival status	State [1]	Collection year	SRA	BioSample
1	1	1_1_A	Wantirna South	70	None (untreated)	0	Control	VIC	2020	SRR15698717	SAMN20863738
2	2	2_2_A	Colbinabbin Sus	50	None (untreated)	0	Control	VIC	2021	SRR20755205	SAMN30107459
2	2	2_2_B	Colbinabbin Sus	50	None (untreated)	0	Control	VIC	2021	SRR20755204	SAMN30107460
3	3	3_2_A	Colbinabbin Sus	50	None (untreated)	0	Control	VIC	2021	SRR20755193	SAMN30107461
3	3	3_2_B	Colbinabbin Sus	50	None (untreated)	0	Control	VIC	2021	SRR20755182	SAMN30107462
4	4	4_1_A	Colbinabbin Res	50	None (untreated)	0	Control	VIC	2021	SRR20755171	SAMN30107463
4	4	4_1_B	Colbinabbin Res	50	None (untreated)	0	Control	VIC	2021	SRR20755160	SAMN30107464
5	5	5_1_A	Colbinabbin Res	50	None (untreated)	0	Control	VIC	2021	SRR20755149	SAMN30107465
5	5	5_1_B	Colbinabbin Res	50	None (untreated)	0	Control	VIC	2021	SRR20755146	SAMN30107466
6	6	6_2_A	Colbinabbin Sus	40	None (untreated)	3.4	Alive	VIC	2021	SRR20755145	SAMN30107467
6	6	6_2_B	Colbinabbin Sus	40	Dimethoate	3.4	Alive	VIC	2021	SRR20755144	SAMN30107468
7	7	7_2_A	Colbinabbin Sus	40	Dimethoate	3.4	Alive	VIC	2021	SRR20755203	SAMN30107469
7	7	7_2_B	Colbinabbin Sus	40	Dimethoate	3.4	Alive	VIC	2021	SRR20755202	SAMN30107470
8	8	8_1_A	Colbinabbin Sus	50	Dimethoate	3.4	Dead	VIC	2021	SRR20755201	SAMN30107471

8	8	8_1_B	Colbinabbin Sus	50	Dimethoate	3.4	Dead	VIC	2021	SRR20755200	SAMN30107472
9	9	9_2_A	Colbinabbin Sus	50	Dimethoate	3.4	Dead	VIC	2021	SRR20755199	SAMN30107473
9	9	9_2_B	Colbinabbin Sus	50	Dimethoate	3.4	Dead	VIC	2021	SRR20755198	SAMN30107474
10	10	10_2_A	Colbinabbin Res	40	Dimethoate	34	Alive	VIC	2021	SRR20755197	SAMN30107475
10	10	10_2_B	Colbinabbin Res	40	Dimethoate	34	Alive	VIC	2021	SRR20755196	SAMN30107476
11	11	11_2_A	Colbinabbin Res	40	Dimethoate	34	Alive	VIC	2021	SRR20755195	SAMN30107477
11	11	11_2_B	Colbinabbin Res	40	Dimethoate	34	Alive	VIC	2021	SRR20755194	SAMN30107478
12	12	12_1_A	Colbinabbin Res	50	Dimethoate	34	Dead	VIC	2021	SRR20755192	SAMN30107479
12	12	12_1_B	Colbinabbin Res	50	Dimethoate	34	Dead	VIC	2021	SRR20755191	SAMN30107480
13	13	13_1_A	Colbinabbin Res	50	Dimethoate	34	Dead	VIC	2021	SRR20755190	SAMN30107481
13	13	13_1_B	Colbinabbin Res	50	Dimethoate	34	Dead	VIC	2021	SRR20755189	SAMN30107482
18	18	18_X_A	Tambellup	20	Omethoate	5.8	Alive	WA	2019	SRR20755188	SAMN30107483
18	18	18_X_B	Tambellup	20	Omethoate	5.8	Alive	WA	2019	SRR20755187	SAMN30107484
19	19	19_1_A	Tambellup	25	Omethoate	5.8	Dead	WA	2019	SRR20755186	SAMN30107485
19	19	19_1_B	Tambellup	25	Omethoate	5.8	Dead	WA	2019	SRR20755185	SAMN30107486
20	20	20_1_A	Treeton	24	Omethoate	5.8	Alive	WA	2019	SRR20755184	SAMN30107487
20	20	20_1_B	Treeton	24	Omethoate	5.8	Alive	WA	2019	SRR20755183	SAMN30107488
21	21	21_1_A	Treeton	18	Omethoate	5.8	Dead	WA	2019	SRR20755181	SAMN30107489
21	21	21_1_B	Treeton	18	Omethoate	5.8	Dead	WA	2019	SRR20755180	SAMN30107490
26|28 [2]	26	26_2_A	Yongarillup	14	Omethoate	5.8	Alive	WA	2019	SRR20755179	SAMN30107491
26|28 [2]	26	26_2_B	Yongarillup	14	Omethoate	5.8	Alive	WA	2019	SRR20755178	SAMN30107492
26|28 [2]	28	28_2_A	Yongarillup	25	Omethoate	5.8	Alive	WA	2019	SRR20755175	SAMN30107495

26|28 [2]	28	28_2_B	Yongarillup	25	Omethoate	5.8	Alive	WA	2019	SRR20755174	SAMN30107496
27|29 [2]	27	27_2_A	Yongarillup	29	Omethoate	5.8	Dead	WA	2019	SRR20755177	SAMN30107493
27|29 [2]	27	27_2_B	Yongarillup	29	Omethoate	5.8	Dead	WA	2019	SRR20755176	SAMN30107494
27|29 [2]	29	29_2_A	Yongarillup	14	Omethoate	5.8	Dead	WA	2019	SRR20755173	SAMN30107497
27|29 [2]	29	29_2_B	Yongarillup	14	Omethoate	5.8	Dead	WA	2019	SRR20755172	SAMN30107498
32|33 [2]	32	32_X_A	Manjimup	12	Omethoate	0.87	Control	WA	2019	SRR20755170	SAMN30107499
32|33 [2]	32	32_X_B	Manjimup	12	Omethoate	0.87	Control	WA	2019	SRR20755169	SAMN30107500
32|33 [2]	33	33_1_A	Manjimup	10	Omethoate	0.87	Control	WA	2019	SRR20755168	SAMN30107501
32|33 [2]	33	33_1_B	Manjimup	10	Omethoate	0.87	Control	WA	2019	SRR20755167	SAMN30107502
38|39 [2]	38	38_X_A	Manjimup	15	Omethoate	8.7	Alive	WA	2019	SRR20755157	SAMN30107511
38|39 [2]	38	38_X_B	Manjimup	15	Omethoate	8.7	Alive	WA	2019	SRR20755156	SAMN30107512
38|39 [2]	39	39_1_A	Manjimup	15	Omethoate	8.7	Alive	WA	2019	SRR20755155	SAMN30107513
38|39 [2]	39	39_1_B	Manjimup	15	Omethoate	8.7	Alive	WA	2019	SRR20755154	SAMN30107514
40|41 [2]	40	40_1_A	Manjimup	12	Omethoate	8.7	Dead	WA	2019	SRR20755153	SAMN30107515
40|41 [2]	40	40_1_B	Manjimup	12	Omethoate	8.7	Dead	WA	2019	SRR20755152	SAMN30107516
40|41 [2]	41	41_X_A	Manjimup	12	Omethoate	8.7	Dead	WA	2019	SRR20755151	SAMN30107517
40|41 [2]	41	41_X_B	Manjimup	12	Omethoate	8.7	Dead	WA	2019	SRR20755150	SAMN30107518

[1] VIC = Victoria; WA = Western Australia

[2] In the Manjimup and Yongarillup samples, we aggregated different DNA pools from the same population and pesticide treatment to increase the number of pooled diploid individuals